Supporting Information

Mechanistic Studies of Adamantylacetophenones with Competing Reaction Pathways in Solution and in the Crystalline Solid State

Vince M. Hipwell and Miguel A. Garcia-Garibay*

Department of Chemistry and Biochemistry, University of California, Los Angeles, California 90095-1569, United States

*e-mail: mgg@chem.ucla.edu

Contents: **Page Number**

Figure S1. ^{1}H NMR (500 MHz, $CDCl_3$) of **1**.

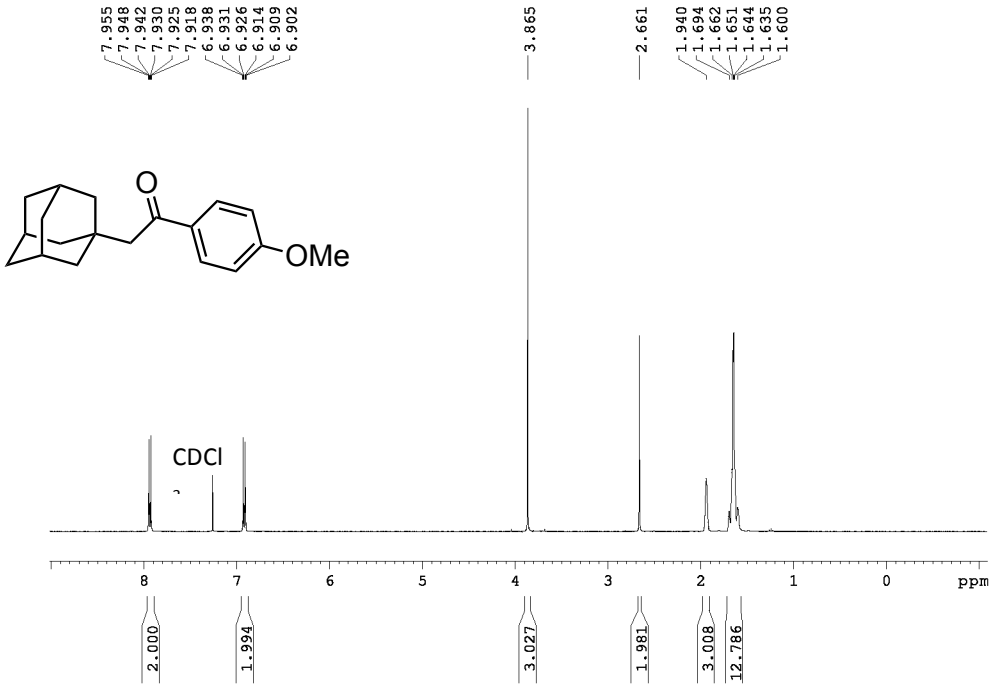

Figure S2. $^{13}C\{^{1}H\}$ NMR (126 MHz, $CDCl_3$) of **1**.

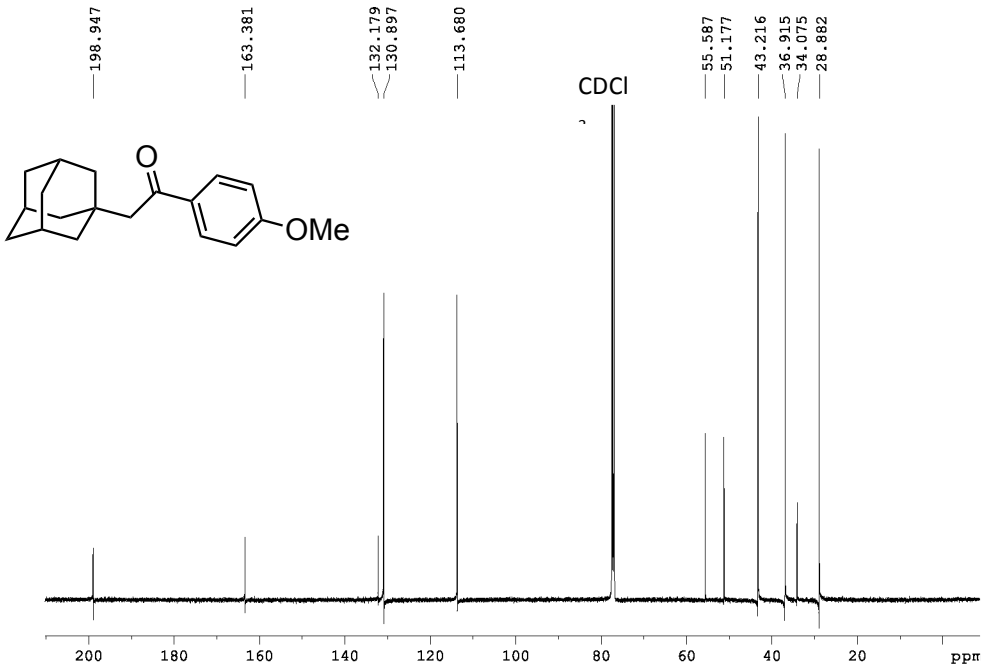

Figure S3. ^{1}H NMR (500 MHz, $CDCl_3$) of **2**.

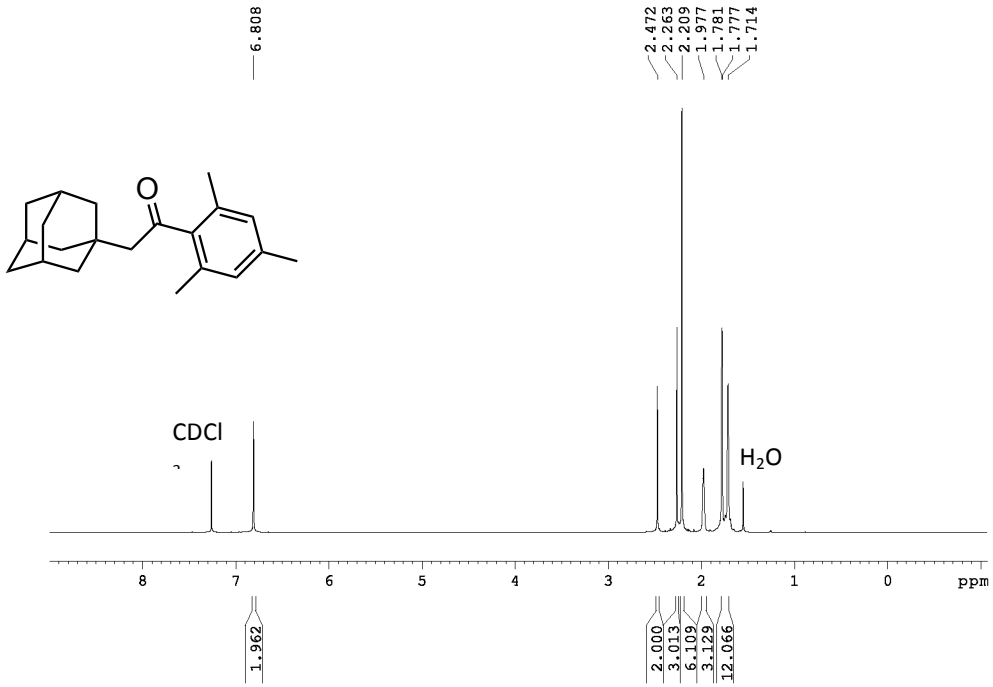

Figure S4. $^{13}C\{^{1}H\}$ NMR (126 MHz, $CDCl_3$) of **2**.

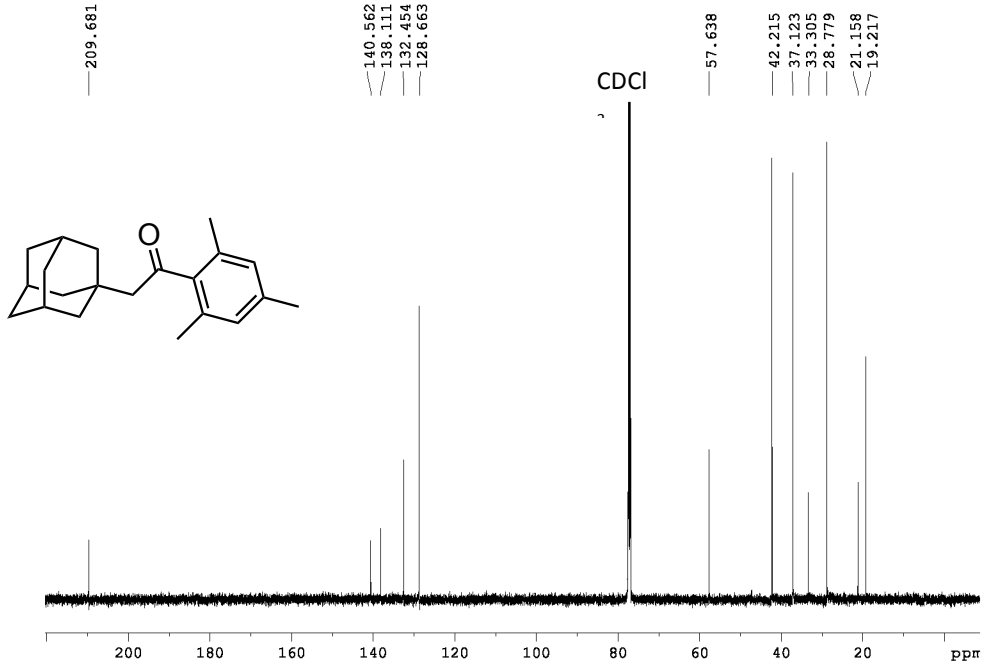

Figure S5. ^{1}H NMR (500 MHz, $CDCl_3$) of **8**.

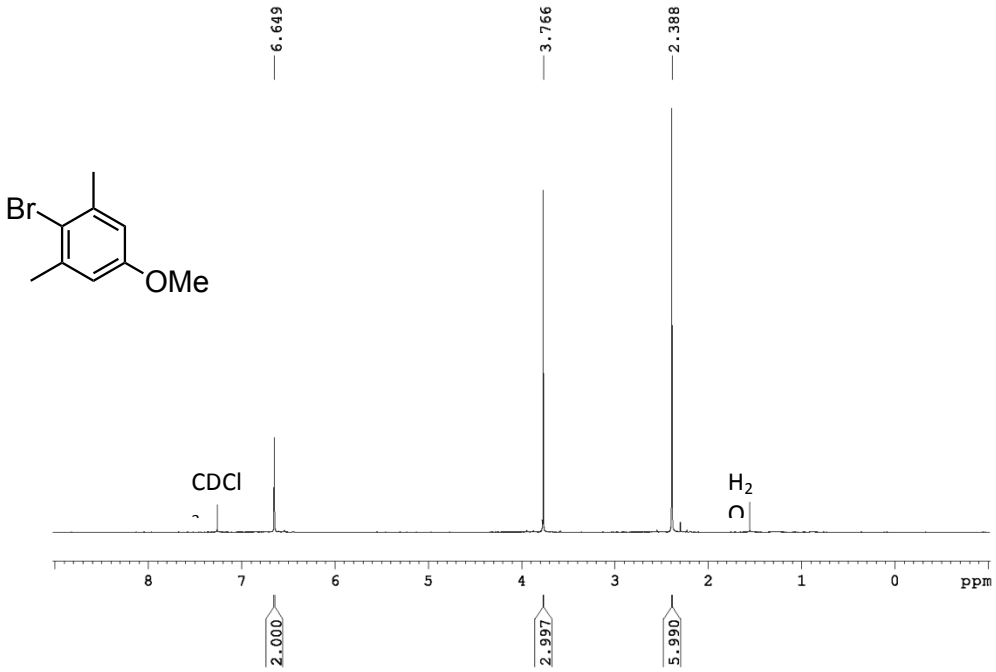

Figure S6. $^{13}C\{^{1}H\}$ NMR (126 MHz, $CDCl_3$) of **8**.

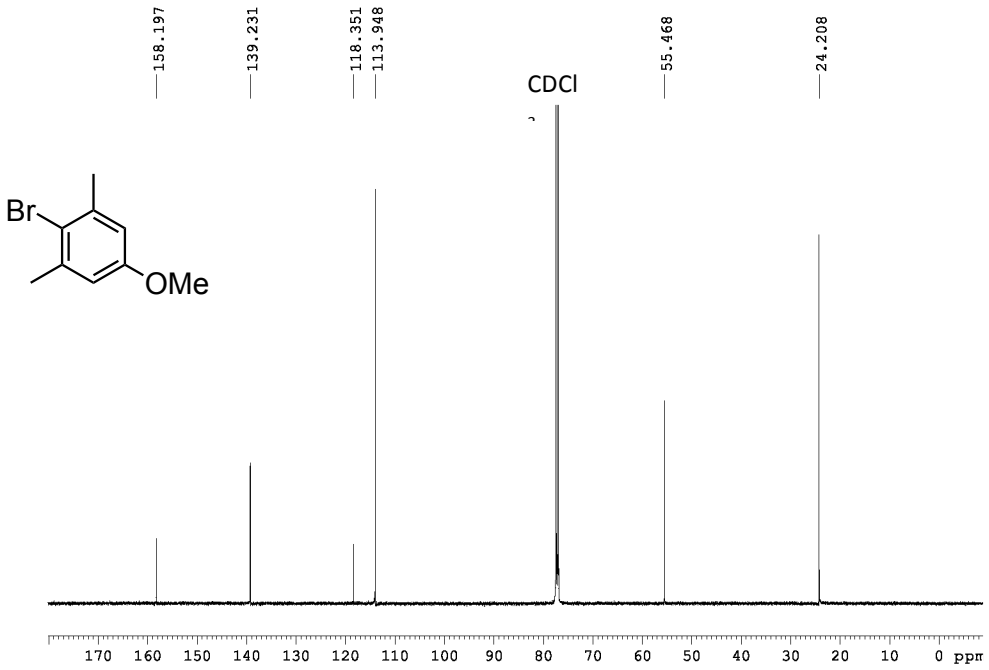

Figure S7. ^{1}H NMR (500 MHz, $CDCl_3$) of **3**.

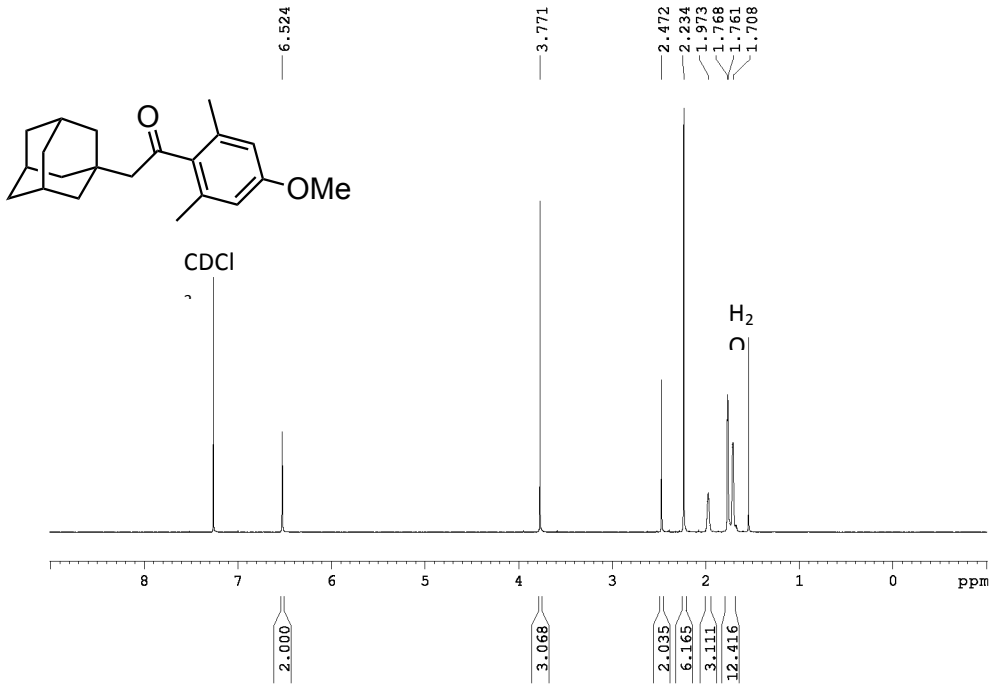

Figure S8. $^{13}C\{^{1}H\}$ NMR (126 MHz, $CDCl_3$) of **3**.

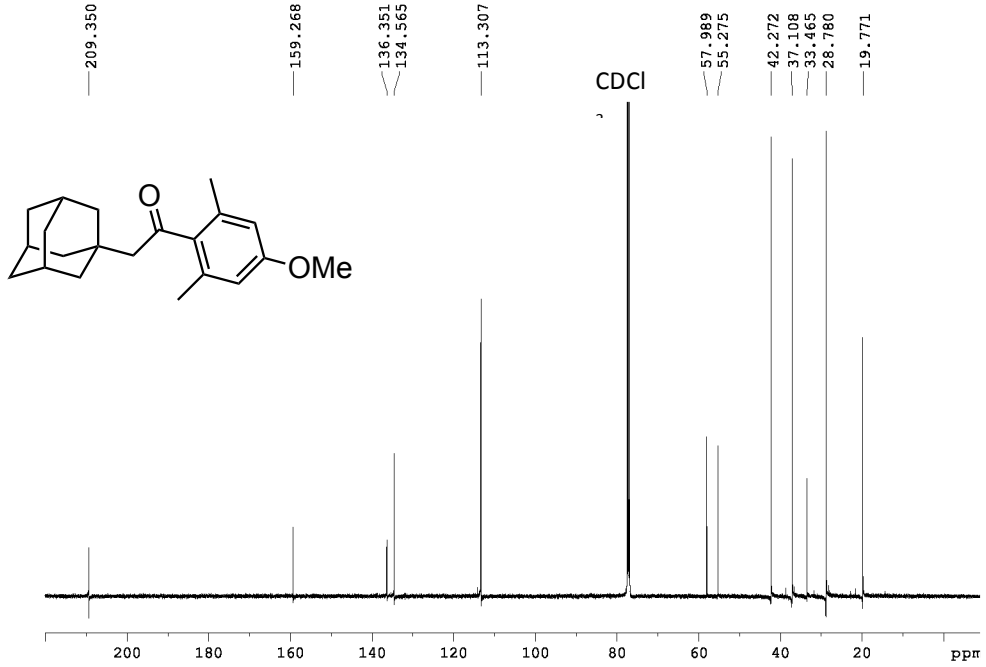

Figure S9. ^{1}H NMR (500 MHz, $CDCl_3$) of **4**.

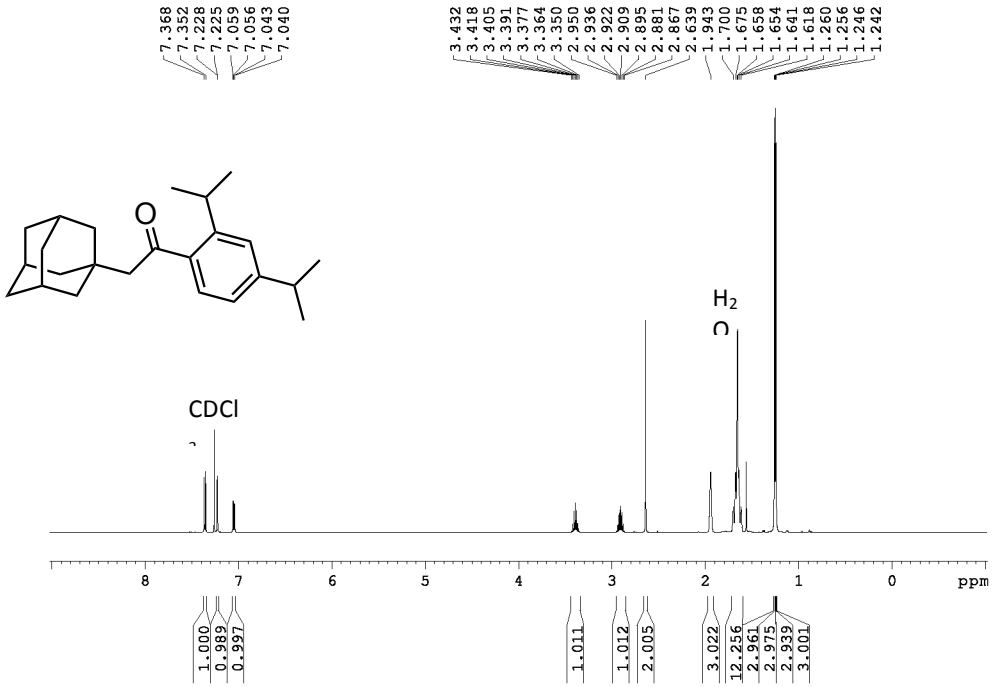

Figure S10. $^{13}C\{^{1}H\}$ NMR (126 MHz, $CDCl_3$) of **4**.

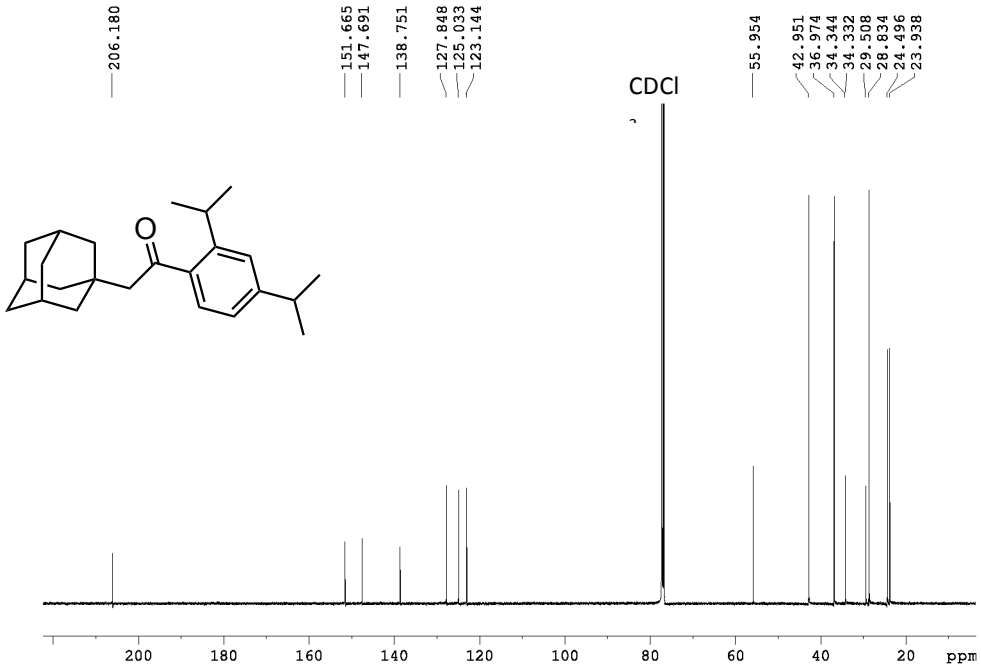

Figure S11. ^{1}H NMR (500 MHz, $CDCl_3$) of **9**.

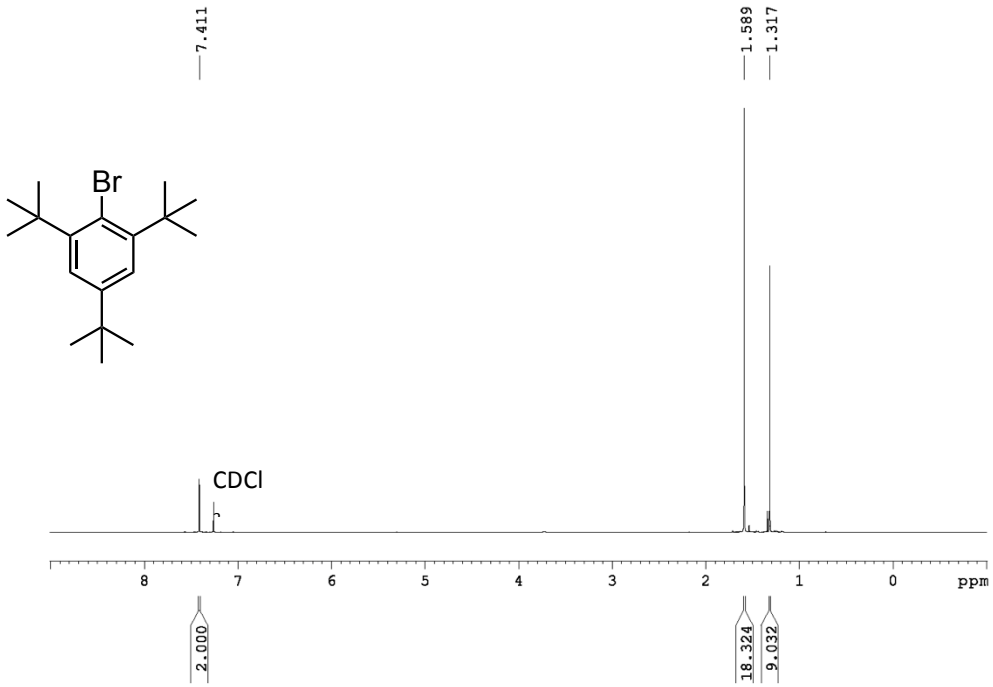

Figure S12. $^{13}C\{^{1}H\}$ NMR (126 MHz, $CDCl_3$) of **9**.

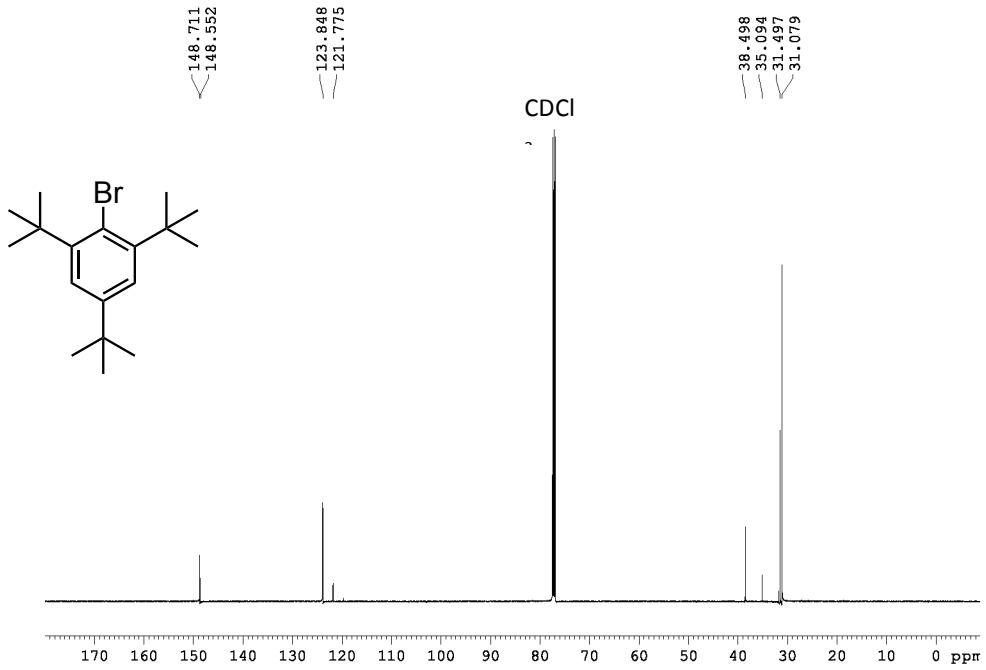

Figure S13. ^{1}H NMR (500 MHz, $CDCl_3$) of **5**.

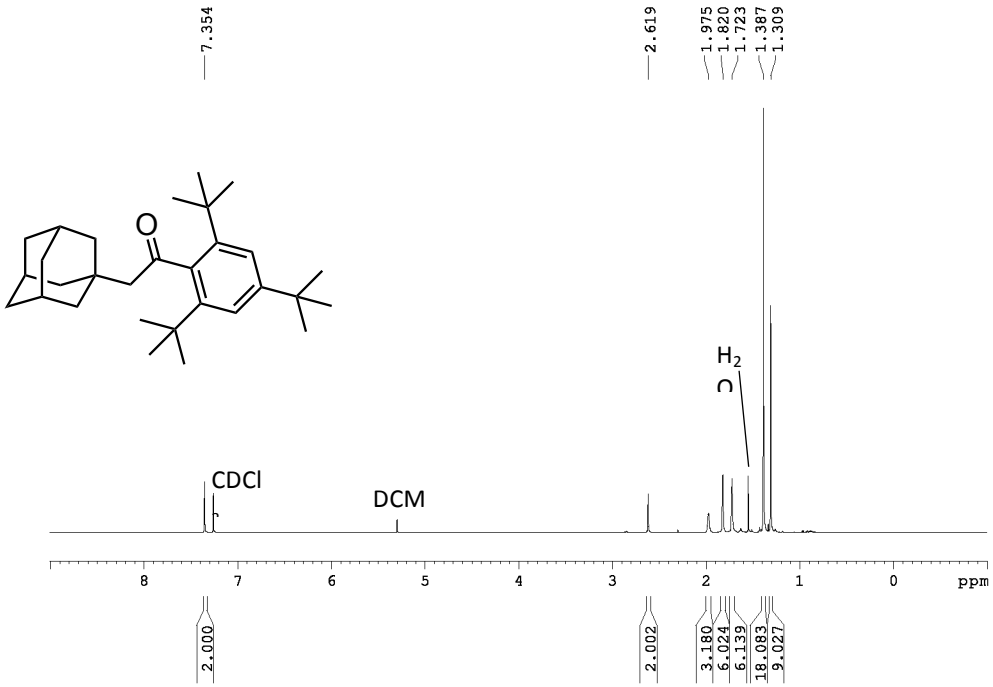

Figure S14. $^{13}C\{^{1}H\}$ NMR (126 MHz, $CDCl_3$) of **5**.

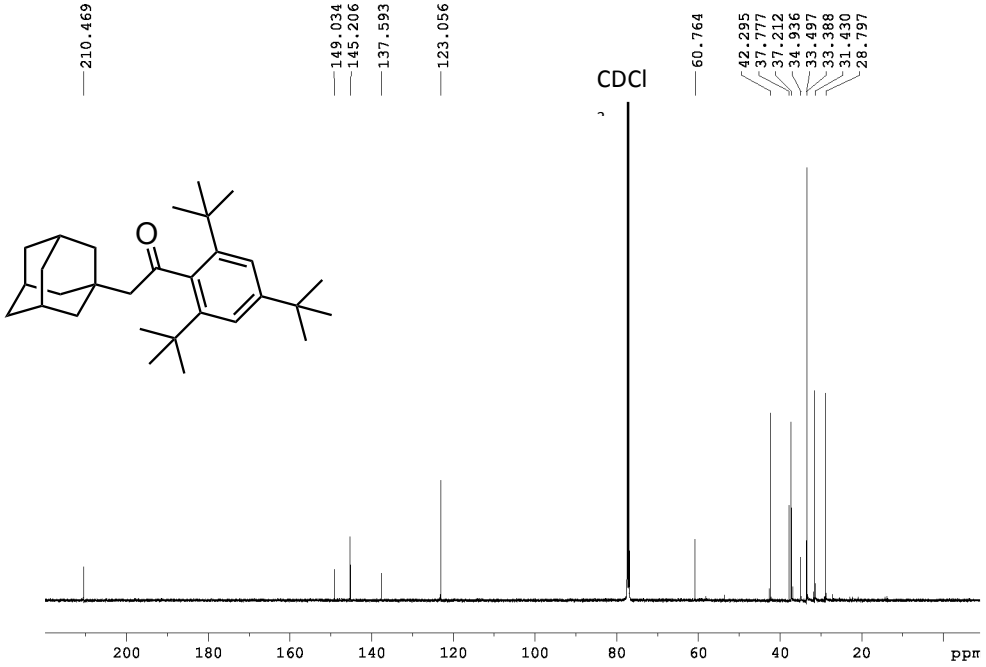

Figure S15. ^{1}H NMR (500 MHz, $CDCl_3$) of **10**.

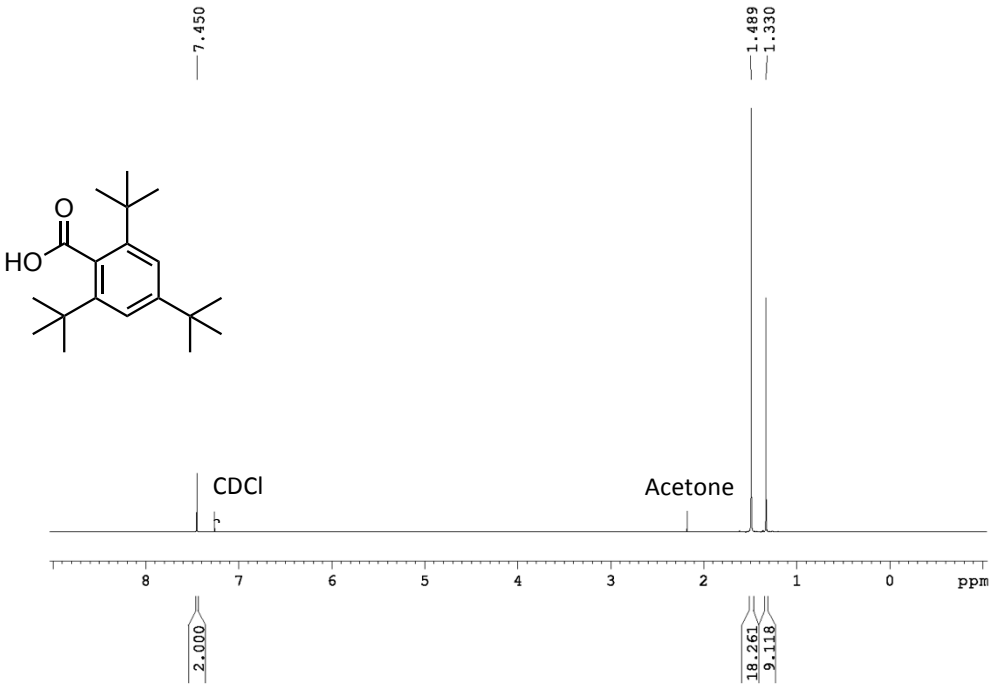

Figure S16. $^{13}C\{^{1}H\}$ NMR (126 MHz, $CDCl_3$) of **10**.

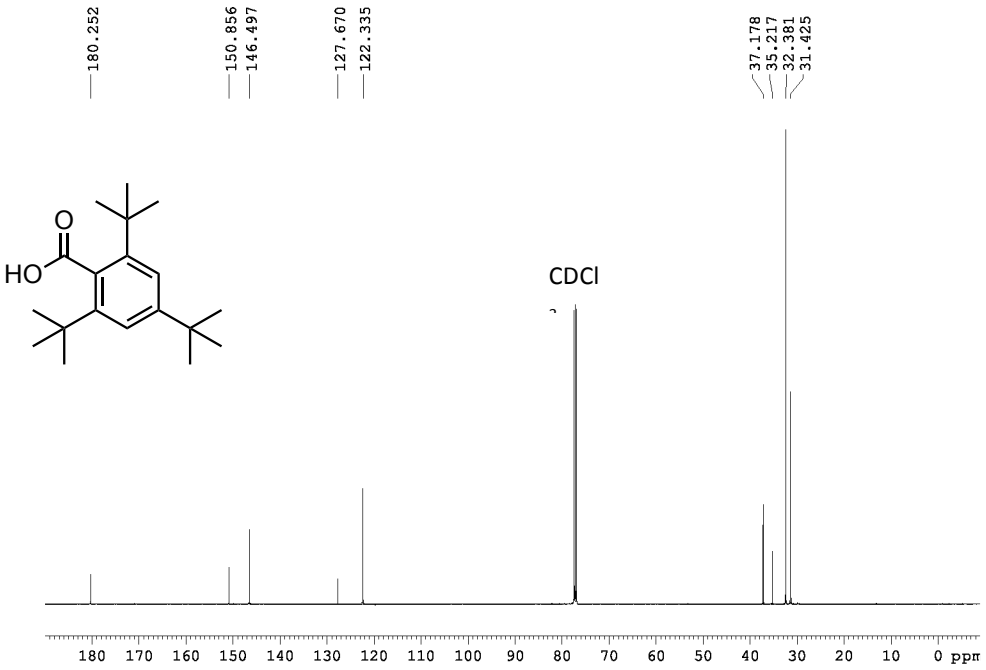

Figure S17. ^{1}H NMR (500 MHz, $CDCl_3$) of **6**.

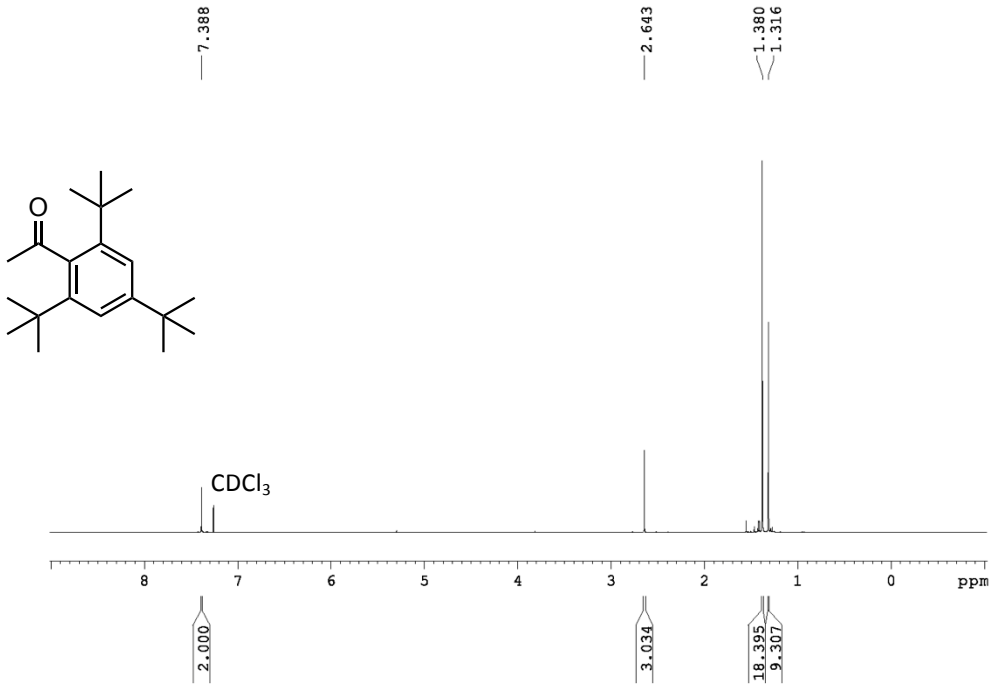

Figure S18. $^{13}C\{^{1}H\}$ NMR (126 MHz, $CDCl_3$) of **6**.

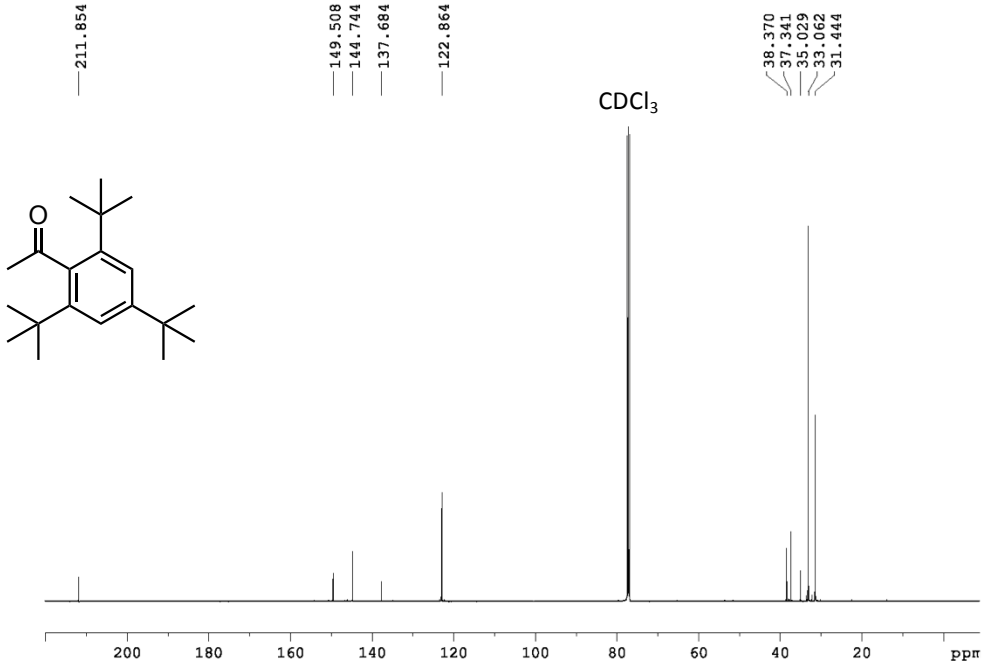

Figure S19. ^{1}H NMR (500 MHz, $CDCl_3$) of **7**.

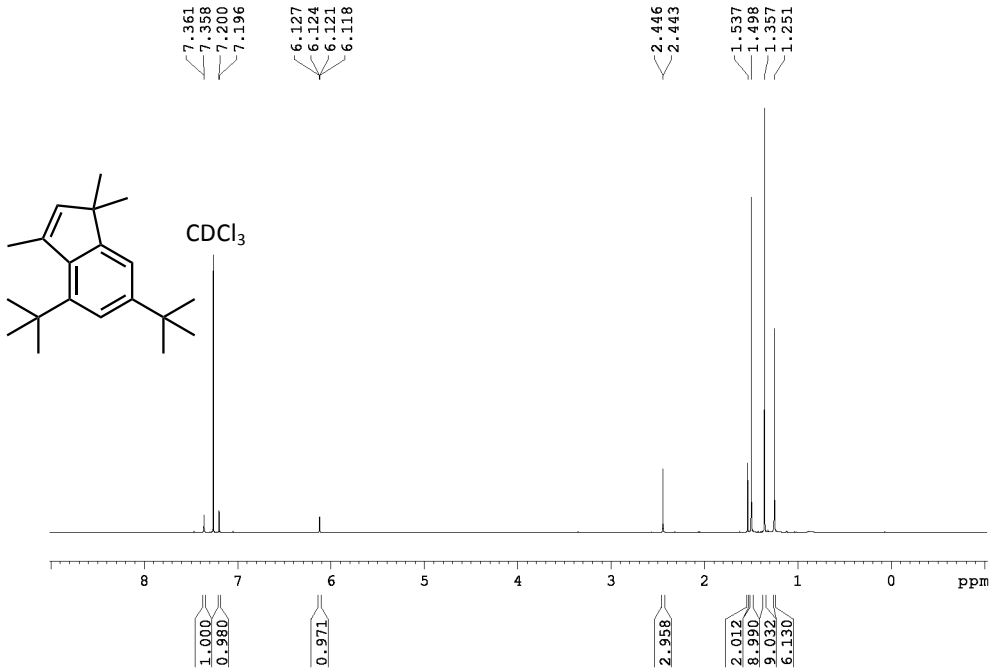

Figure S20. $^{13}C\{^{1}H\}$ NMR (126 MHz, $CDCl_3$) of **7**.

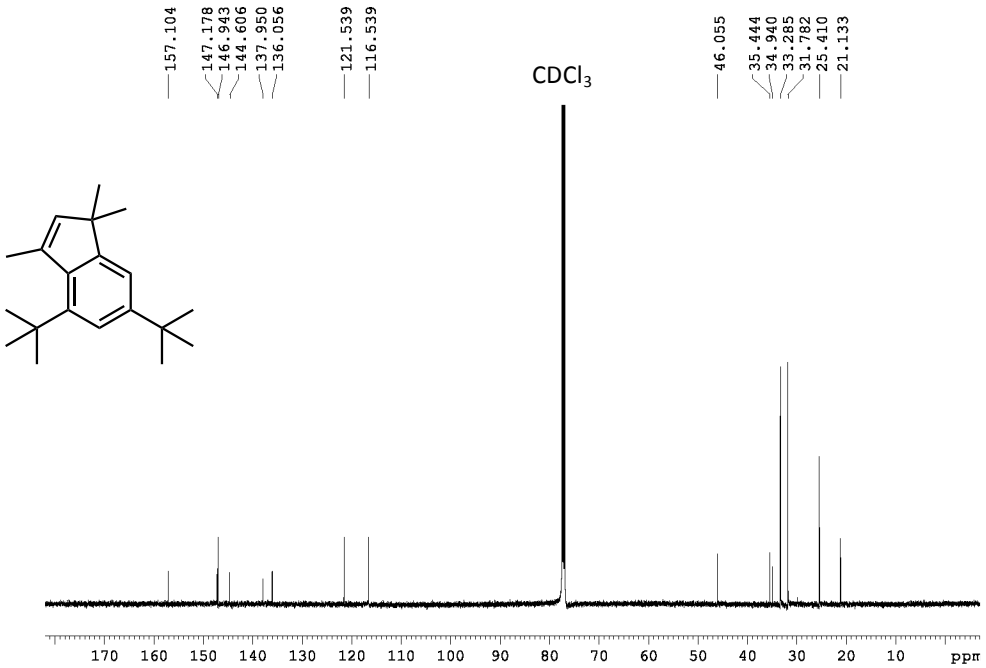

Figure S21. IR (powder) of **1**.

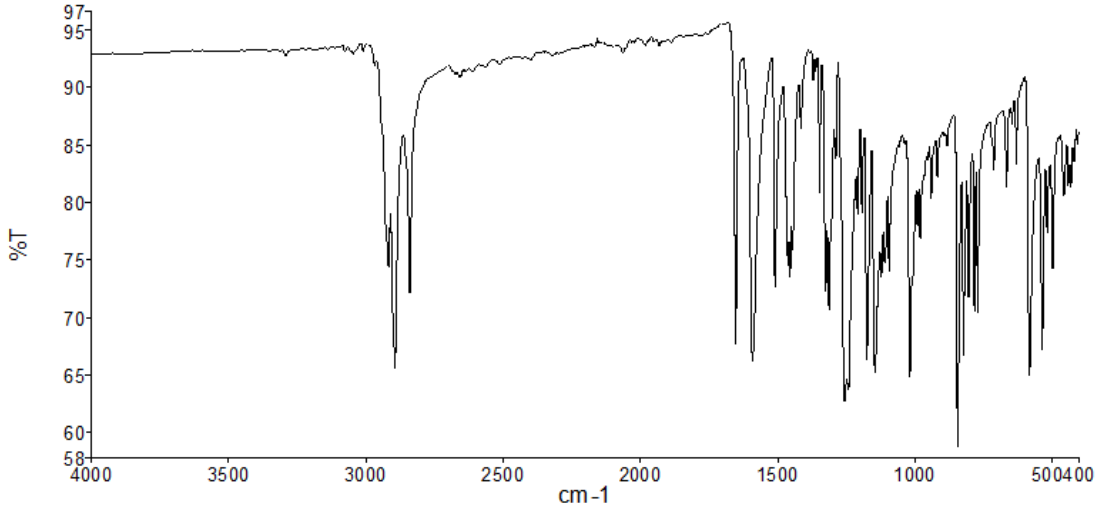

Figure S22. IR (film) of **2**.

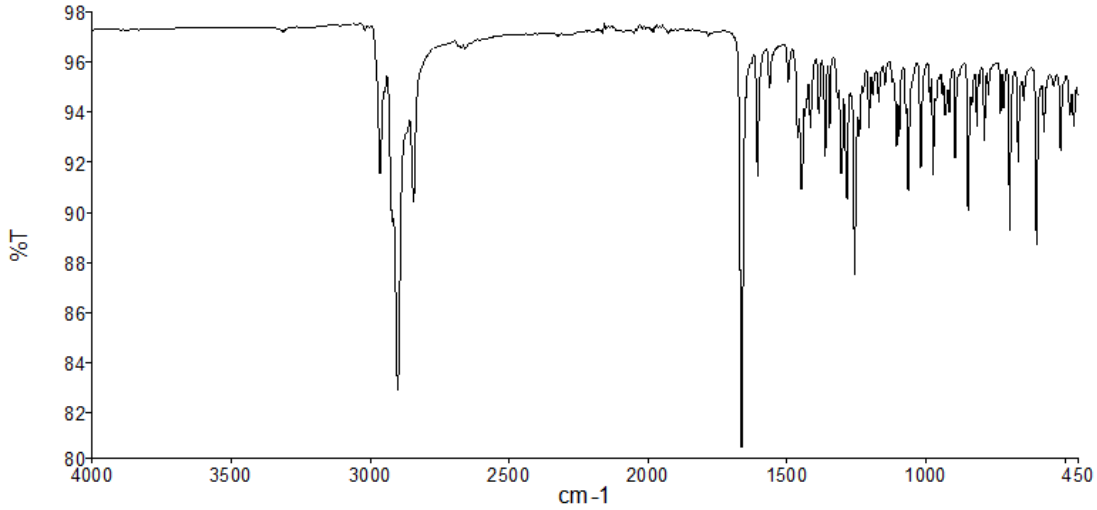

Figure S23. IR (film) of **8**.

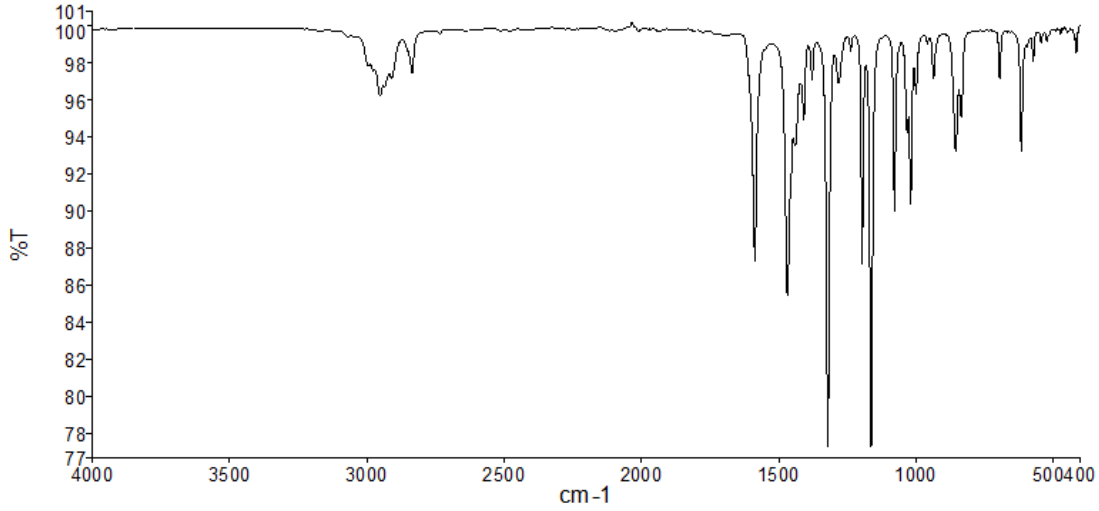

Figure S24. IR (film) of **3**.

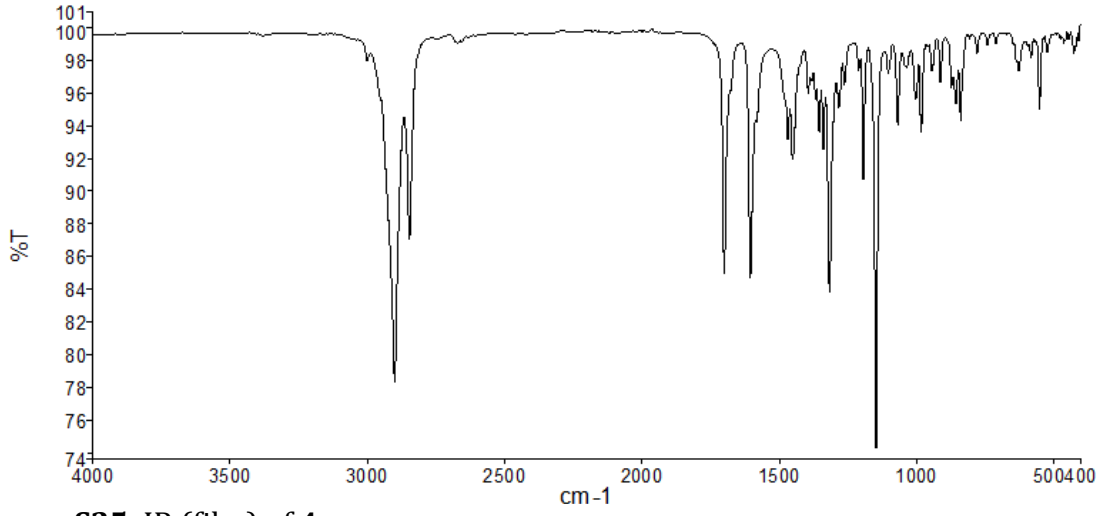

Figure S25. IR (film) of **4**.

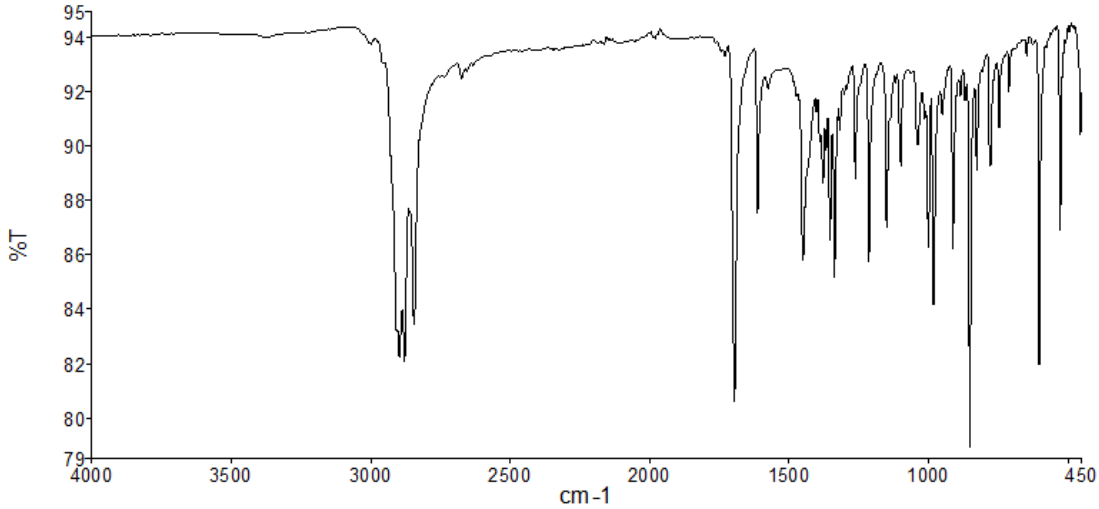

Figure S26. IR (powder) of **9**.

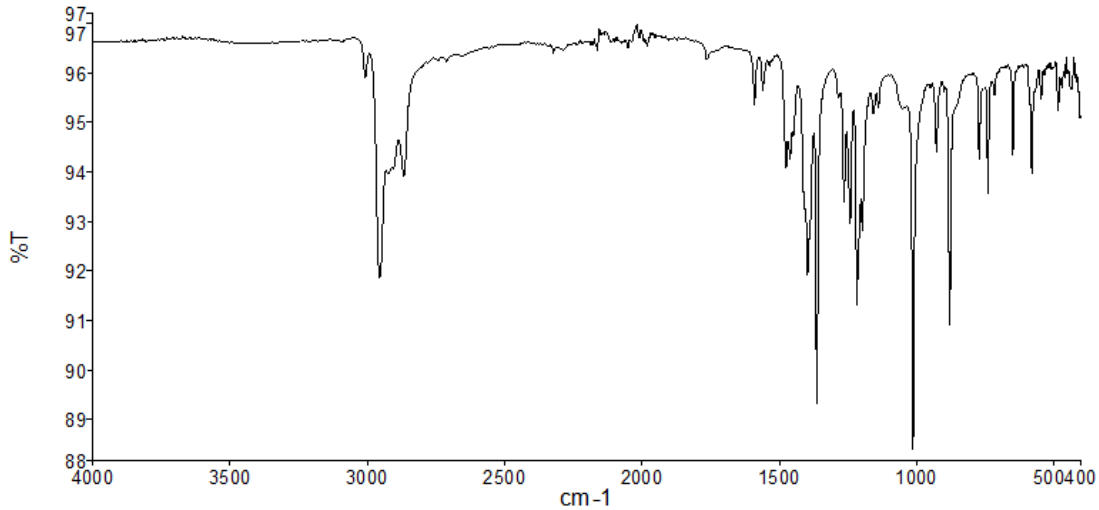

Figure S27. IR (film) of **5**.

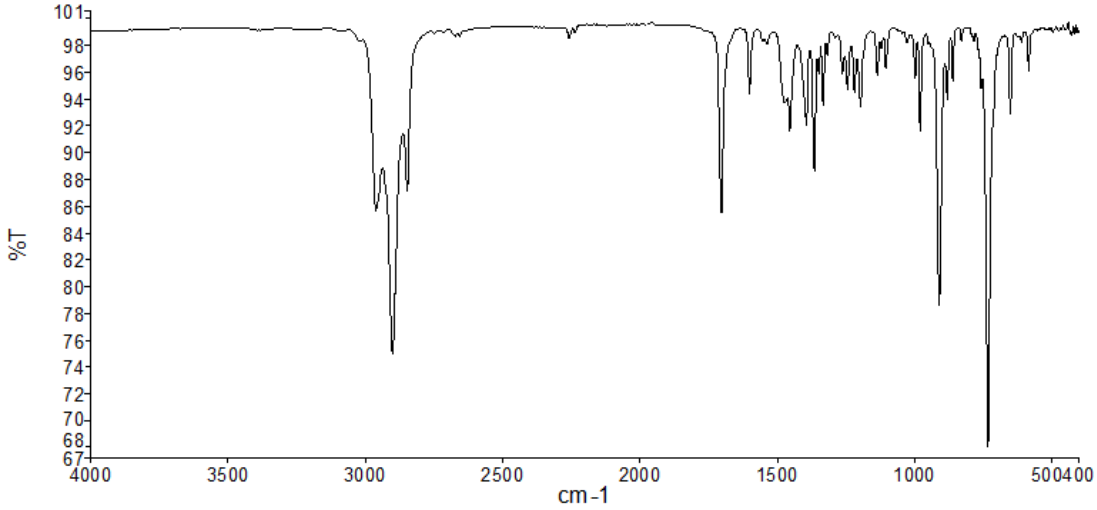

Figure S28. IR (film) of **10**.

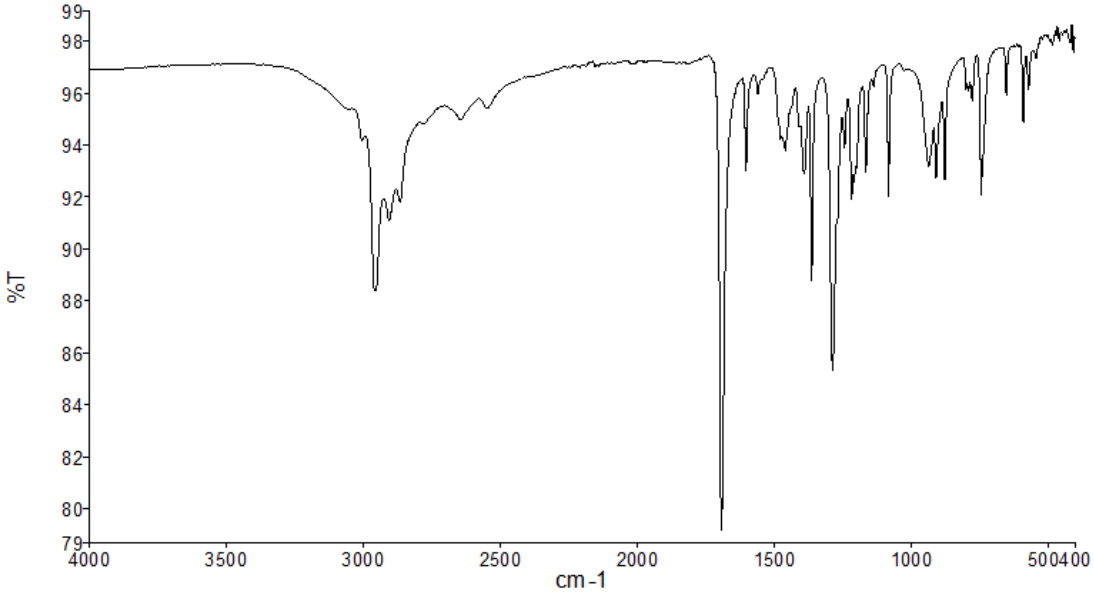

Figure S29. IR (film) of **6**.

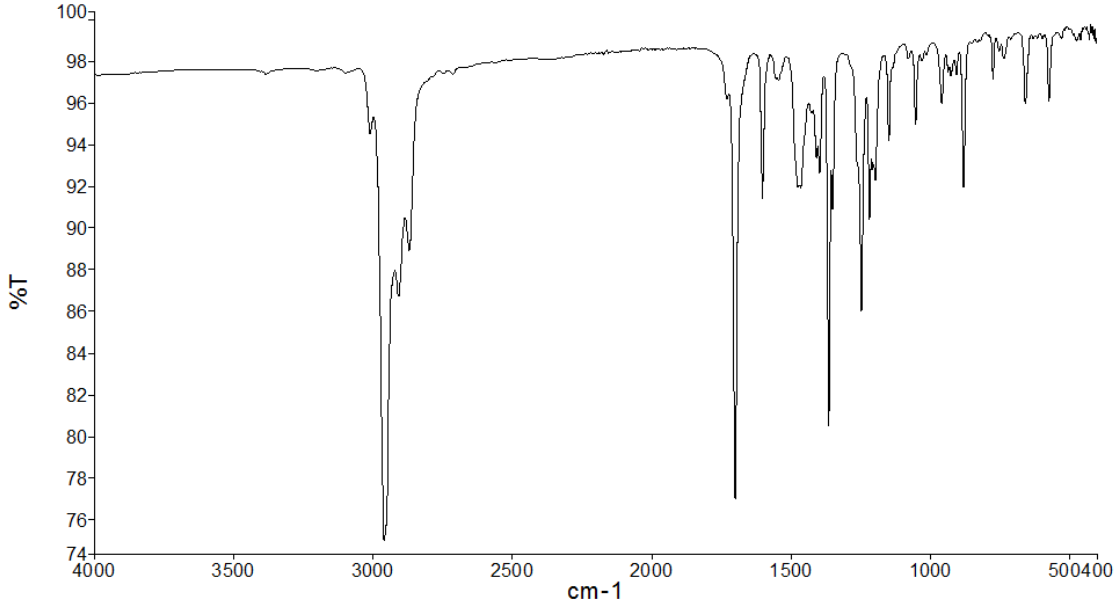

Figure S30. IR (film) of **7**.

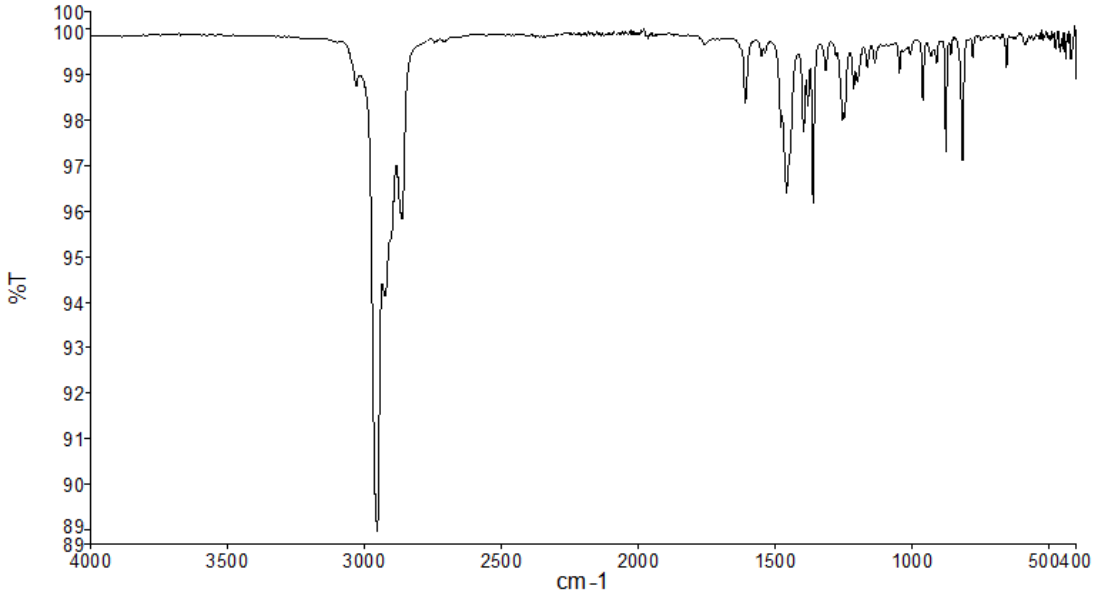

Figure S31. UV-Vis Spectra of **1** : 0.01 mg/mL MeCN solution and 0.01 mg/mL nanocrystalline suspension at 0, 10, 20, and 30 minutes.

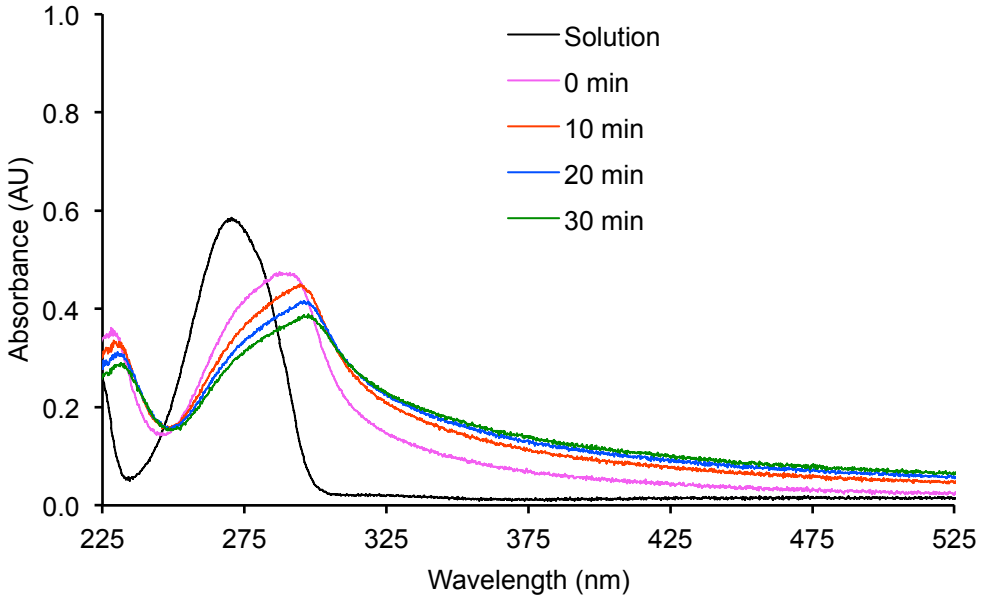

Figure S32. UV-Vis Spectra of **2** : 0.05 mg/mL MeCN solution and 0.05 mg/mL nanocrystalline suspension at 0, 10, 20, and 30 minutes.

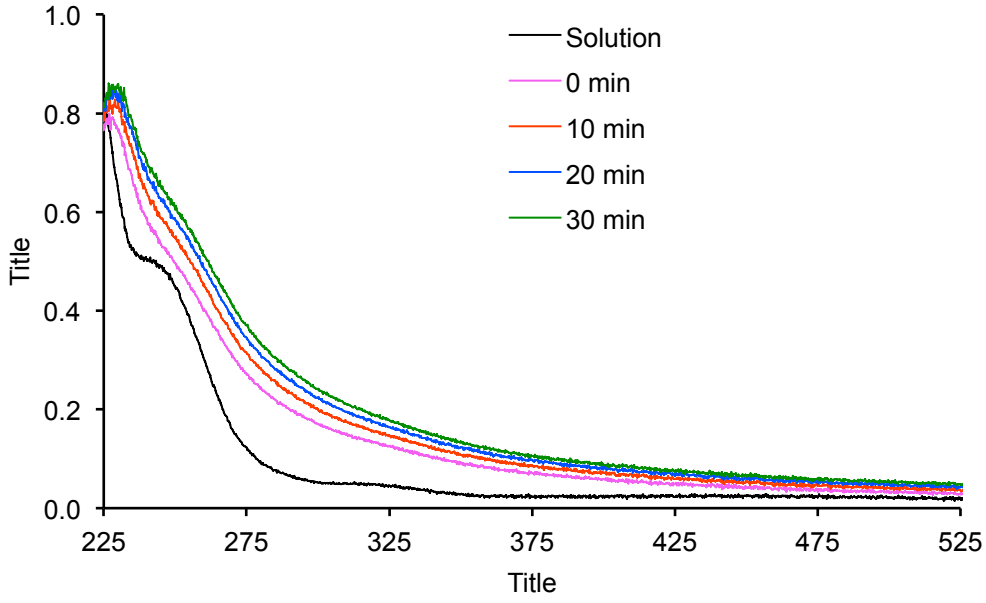

Figure S33. UV-Vis Spectra of **3** : 0.02 mg/mL MeCN solution and 0.02 mg/mL nanocrystalline suspension at 0, 10, 20, and 30 minutes.

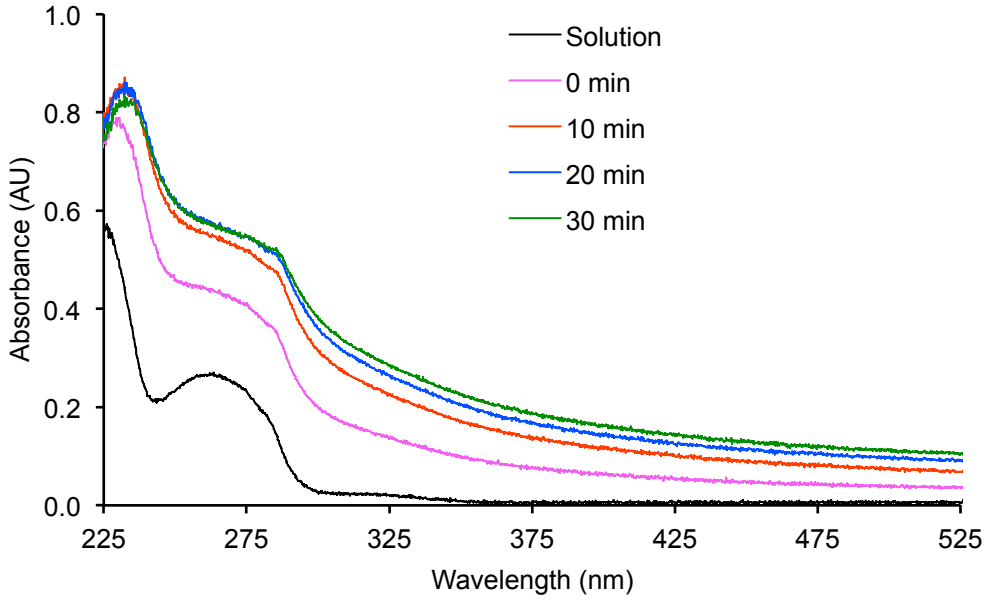

Figure S34. UV-Vis Spectra of **4** : 0.025 mg/mL MeCN solution and 0.025 mg/mL nanocrystalline suspension at 0, 10, 20, and 30 minutes.

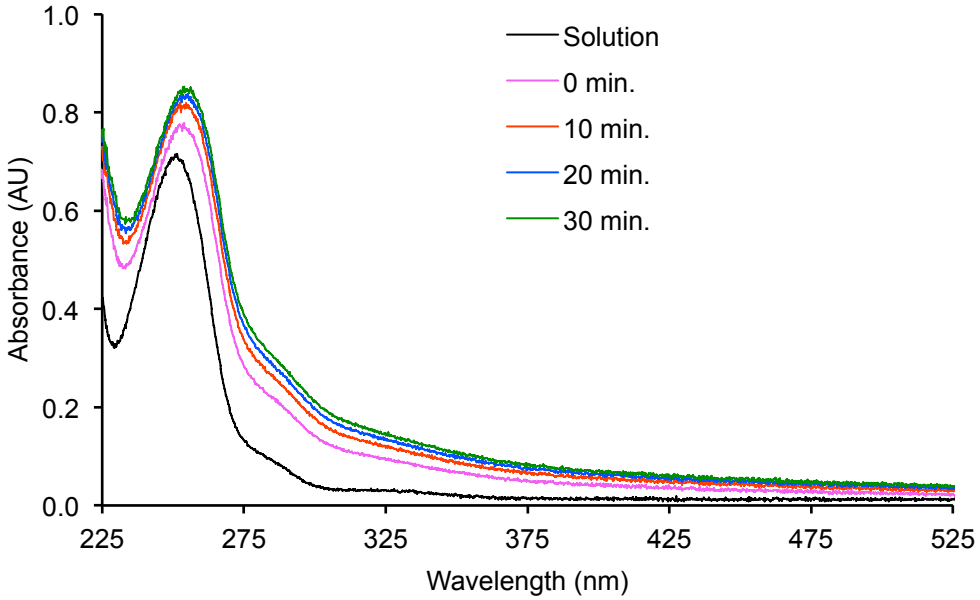

Figure S35. UV-Vis Spectra of **5** : 0.05 mg/mL MeCN solution and 0.05 mg/mL nanocrystalline suspension at 0, 10, 20, and 30 minutes.

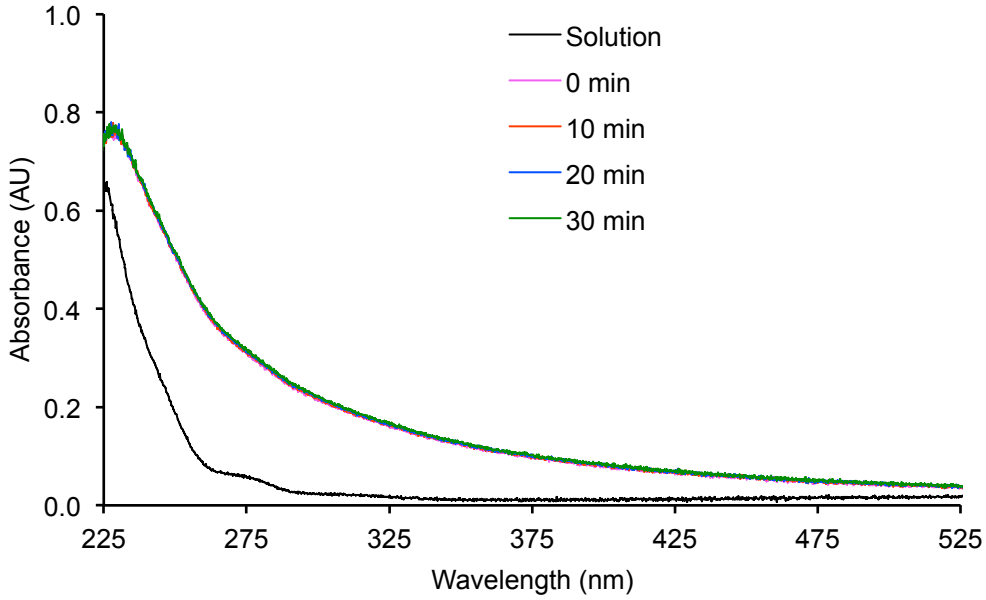

Figure S36. Phosphorescence spectrum of **1** : 0.01 mg/mL in methylcyclohexane at 77 K.

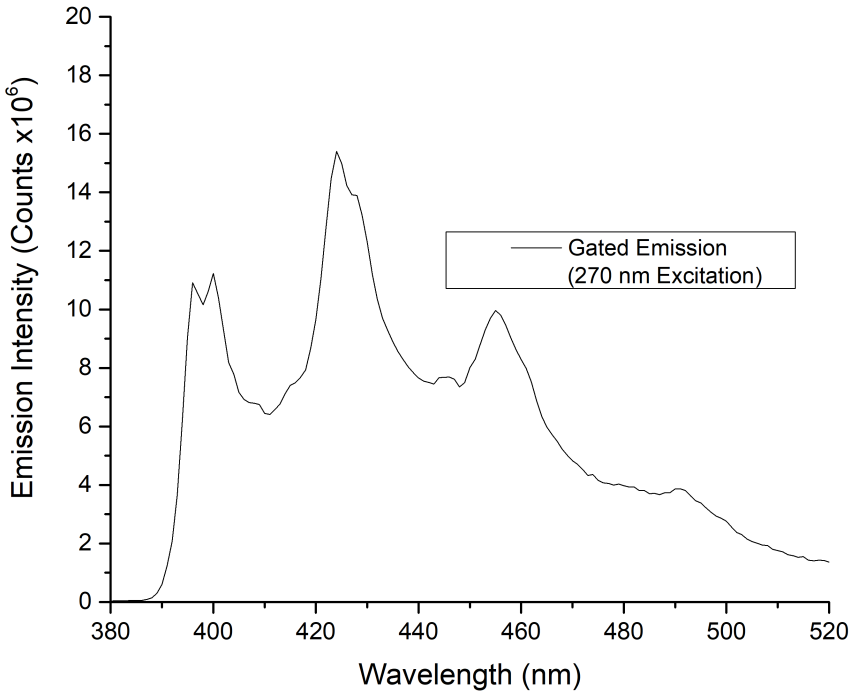

Figure S37. Phosphorescence spectrum of **2** : 0.05 mg/mL in methylcyclohexane at 77 K.

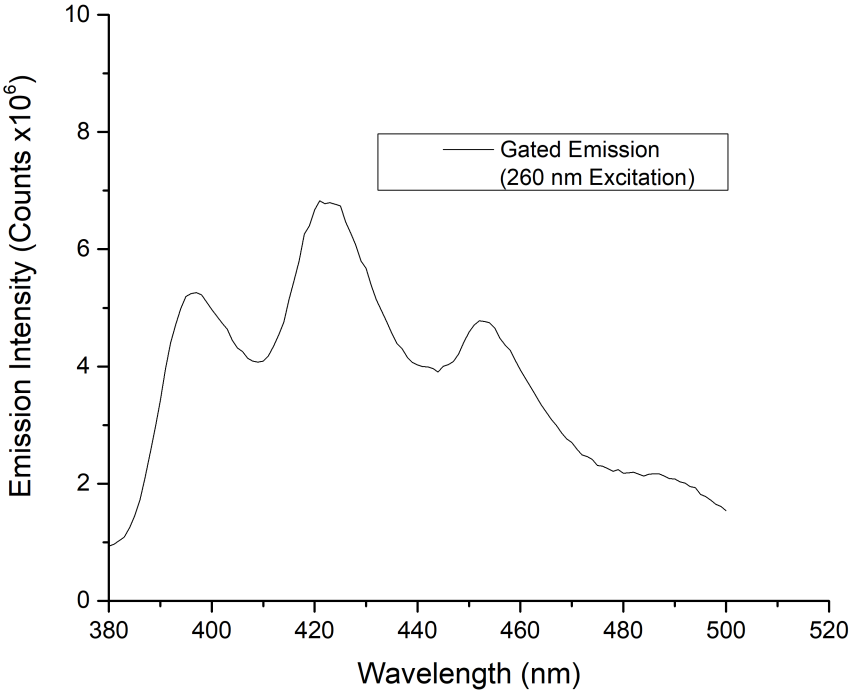

Figure S38. Phosphorescence spectrum of **3** : 0.05 mg/mL in methylcyclohexane at 77 K.

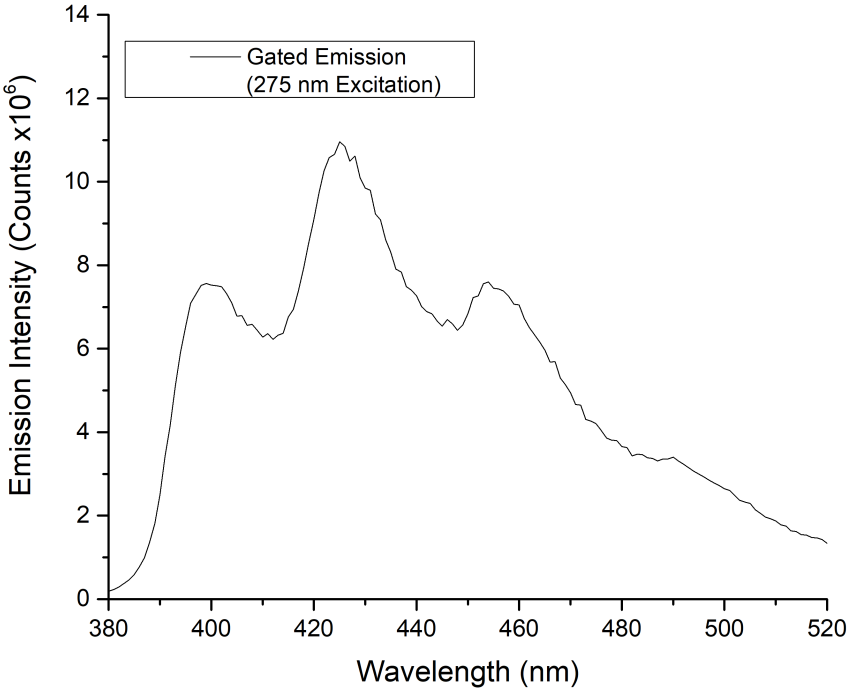

Figure S39. Phosphorescence spectrum of **4** : 0.05 mg/mL in methylcyclohexane at 77 K.

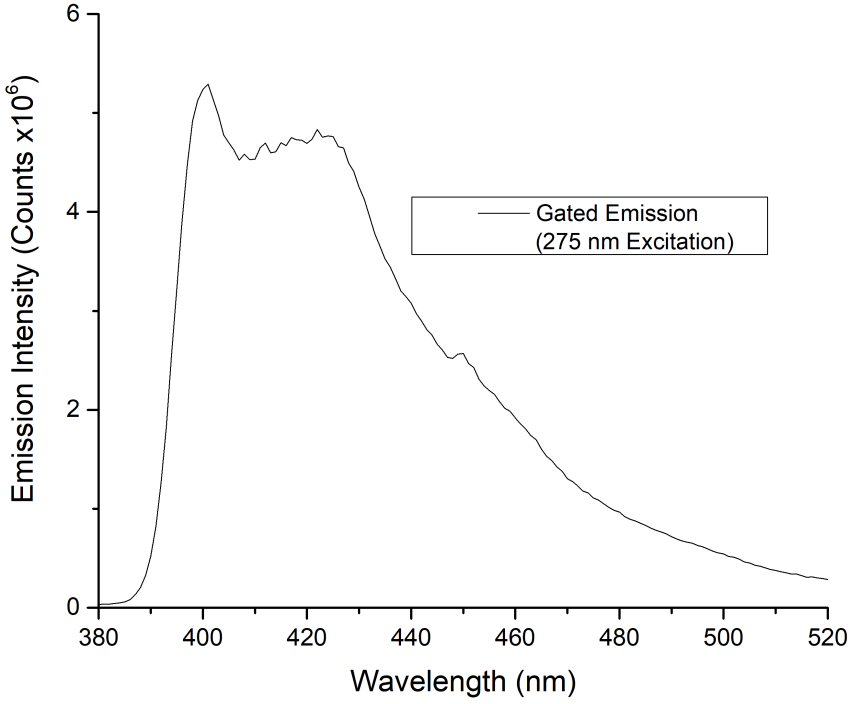

Figure S40. Phosphorescence spectrum of **5** : 0.05 mg/mL in methylcyclohexane at 77 K.

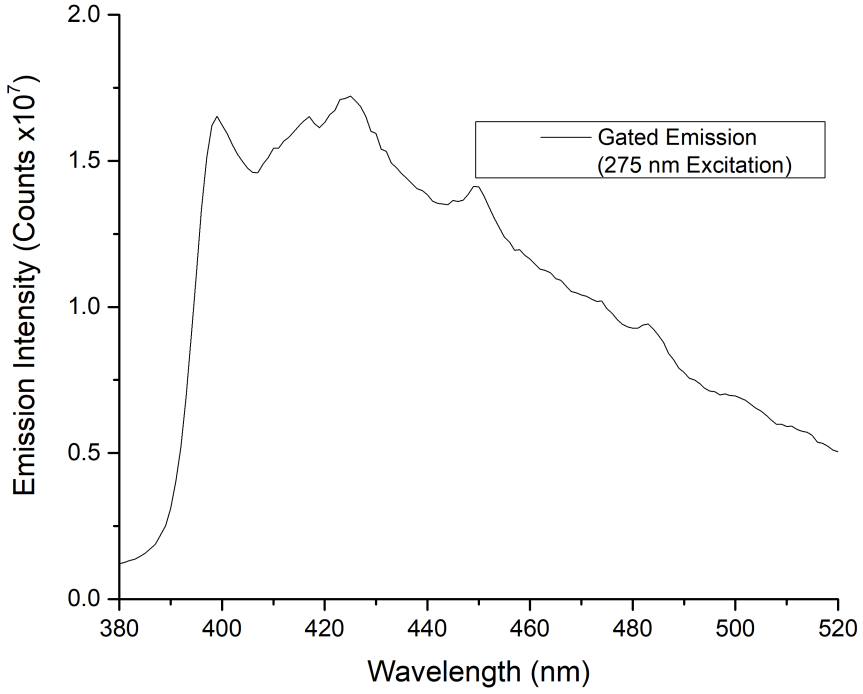

Table S1. Photoproduct distributions of 1-5 in MeCN solutions and aqueous suspensions.

Compound	Medium	Reaction Time (min.)	% Conversion	% *cis*-ACB	% *trans*-ACB	% BCB	% Deuteration
1	MeCN	10	29	36	64	N/A	N/A
		120	96	38	62	N/A	N/A
	Suspension	10	47	75	25	N/A	N/A
		120	72	69	31	N/A	N/A
2	MeCN	10	2	0	0	100	4
		120	26	0	0	100	13
	Suspension	10	5	0	0	100	N/A
		120	43	0	0	100	N/A
3	MeCN	10	<1	<1	<1	0	0
		120	6	70	30	0	0
	Suspension	10	<1	<1	<1	0	N/A
		120	6	78	22	0	N/A
4	MeCN	10	5	41	18	41	5
		120	21	16	21	63	23
	Suspension	10	6	24	28	48	N/A
		120	22	13	49	37	N/A
5	MeCN	10	0	0	0	0	N/A
		120	0	0	0	0	N/A
	Suspension	10	0	0	0	0	N/A
		120	0	0	0	0	N/A

Figure S41. ^{1}H NMR (500 MHz, $CDCl_3$) of ***trans*-ACB-1**.

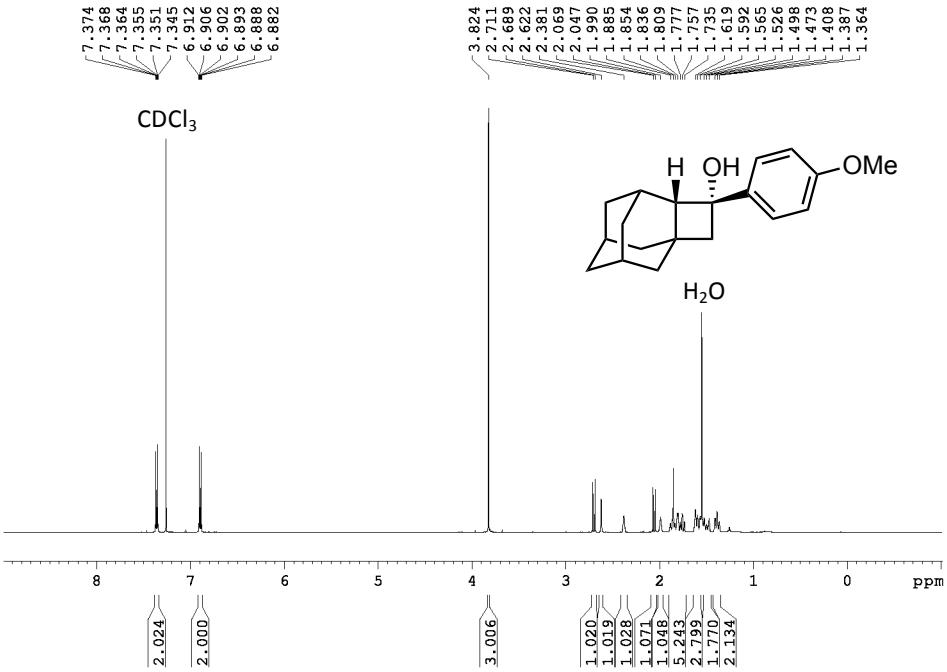

Figure S42. $^{13}C\{^{1}H\}$ NMR (126 MHz, $CDCl_3$) of ***trans*-ACB-1**.

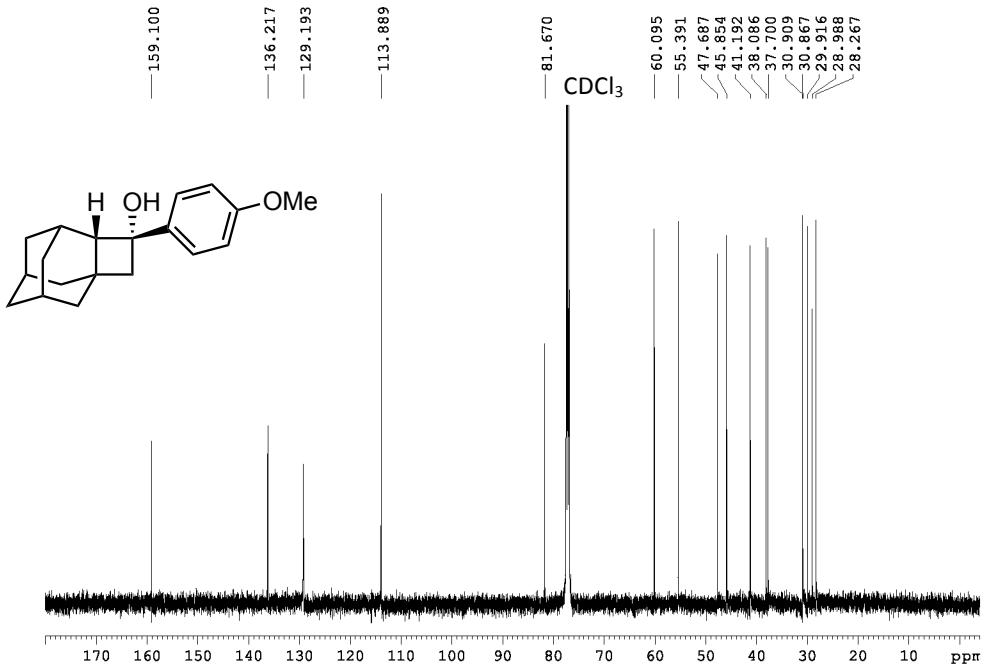

Figure S43. ^{1}H NMR (500 MHz, $CDCl_3$) of ***cis*-ACB-1**.

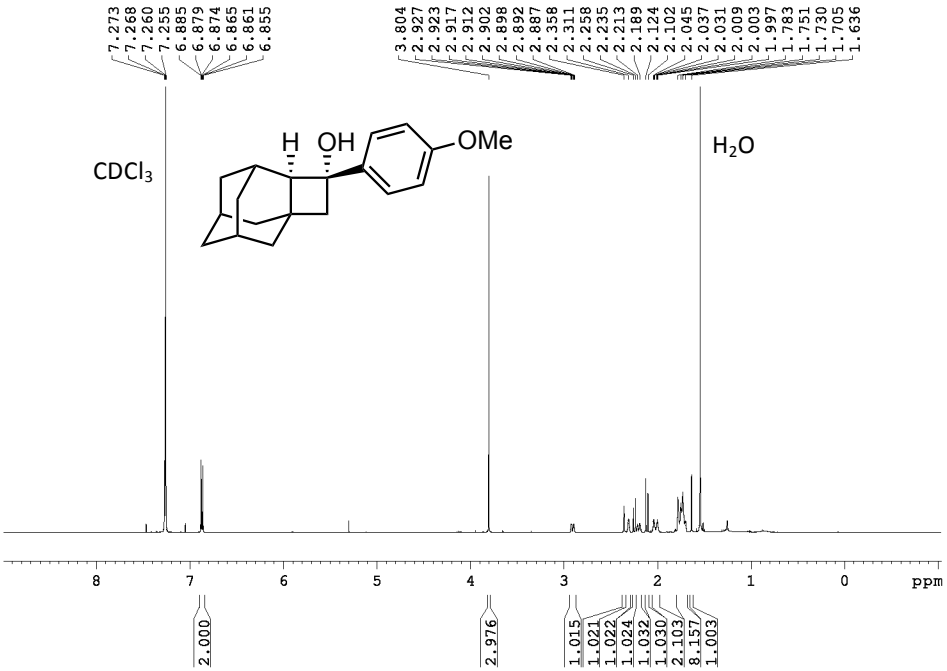

Figure S44. $^{13}C\{^{1}H\}$ NMR (126 MHz, $CDCl_3$) of ***cis*-ACB-1**

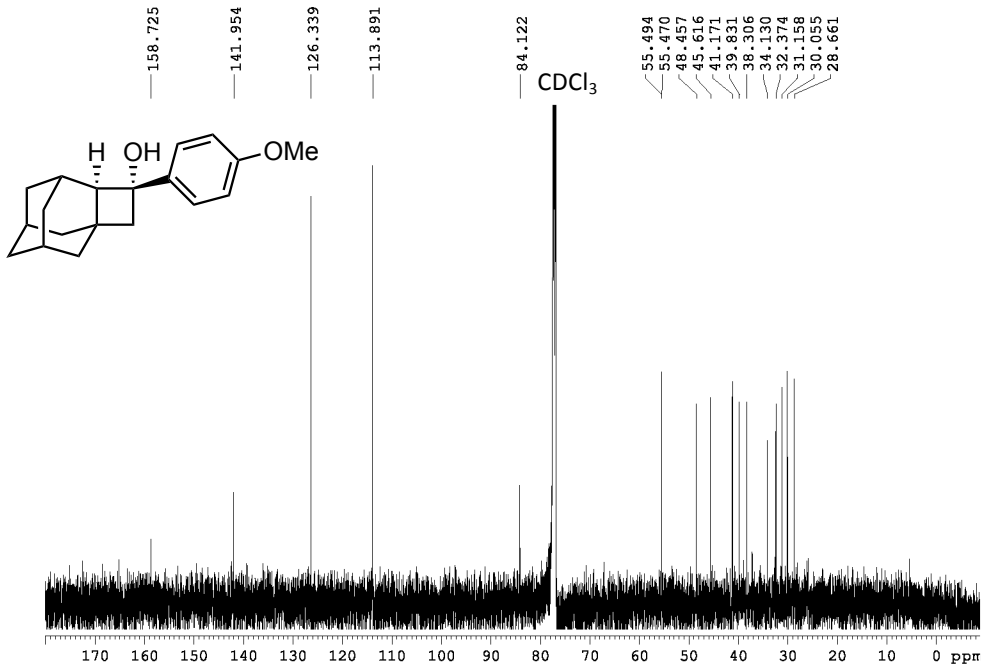

Figure S45. ^{1}H NMR (500 MHz, $CDCl_3$) of **BCB-2**.

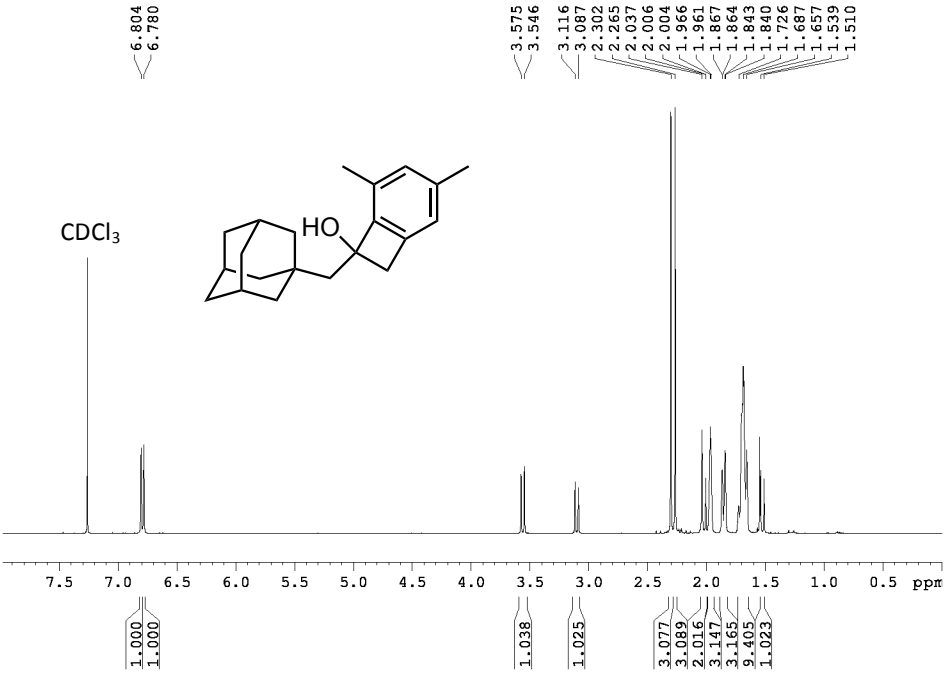

Figure S46. $^{13}C\{^{1}H\}$ NMR (126 MHz, $CDCl_3$) of **BCB-2**.

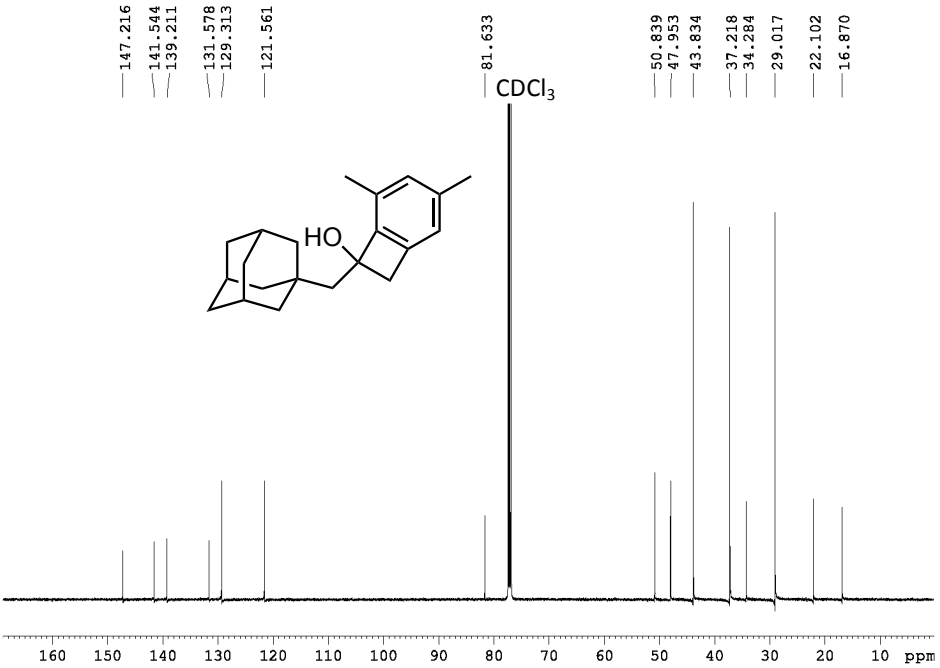

Figure S47. ^{1}H NMR (500 MHz, $CDCl_3$) of elimination product of ***cis-*** and ***trans*-ACB-3**.

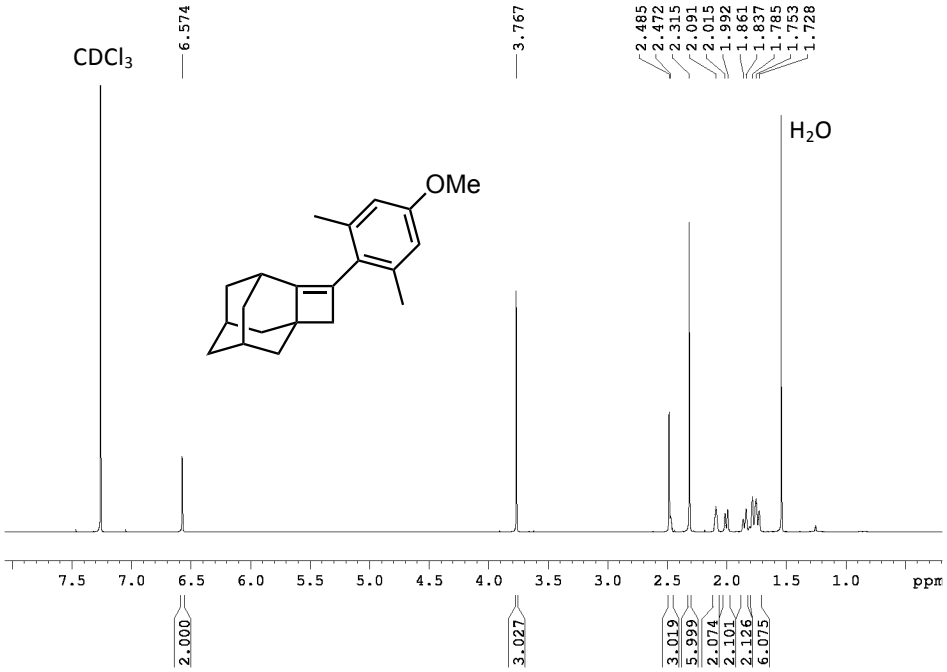

Figure S48. $^{13}C\{^{1}H\}$ NMR (126 MHz, $CDCl_3$) of elimination product of ***cis-*** and ***trans*-ACB-3**.

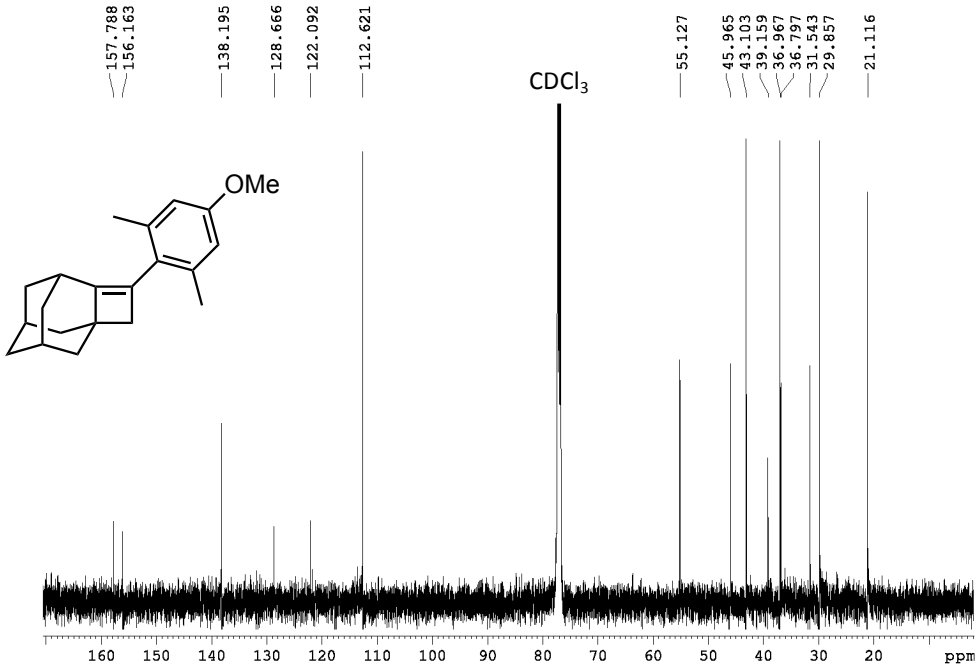

Figure S49. ^{1}H NMR (500 MHz, $CDCl_3$) of elimination product of **BCB-3**.

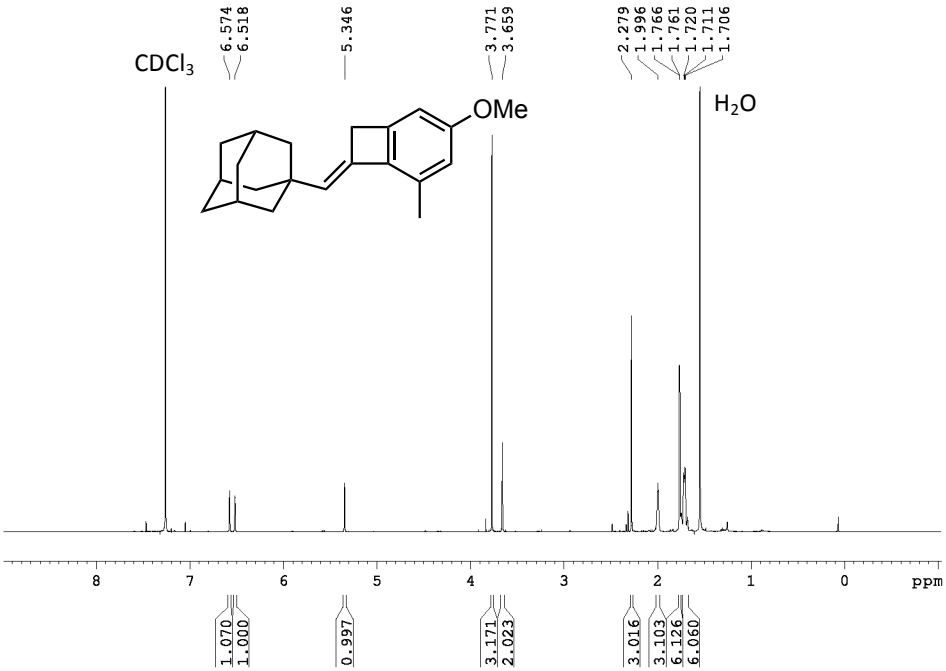

Figure S50. $^{13}C\{^{1}H\}$ NMR (126 MHz, $CDCl_3$) of elimination product of **BCB-3**.

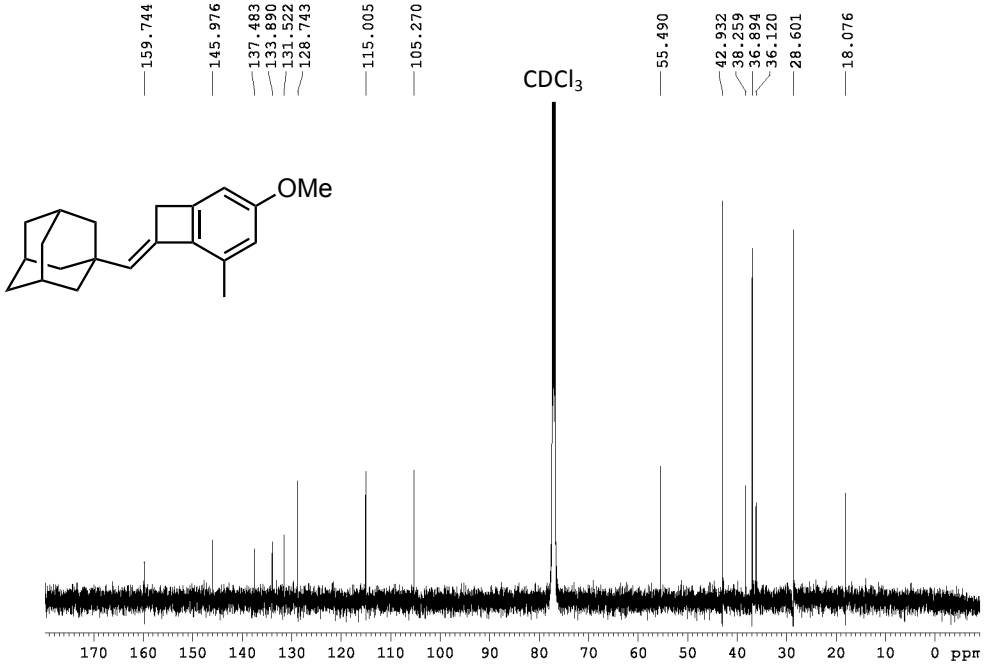

Figure S51. ^{1}H NOESY NMR (500 MHz, $CDCl_3$) of elimination product of **BCB-3**.

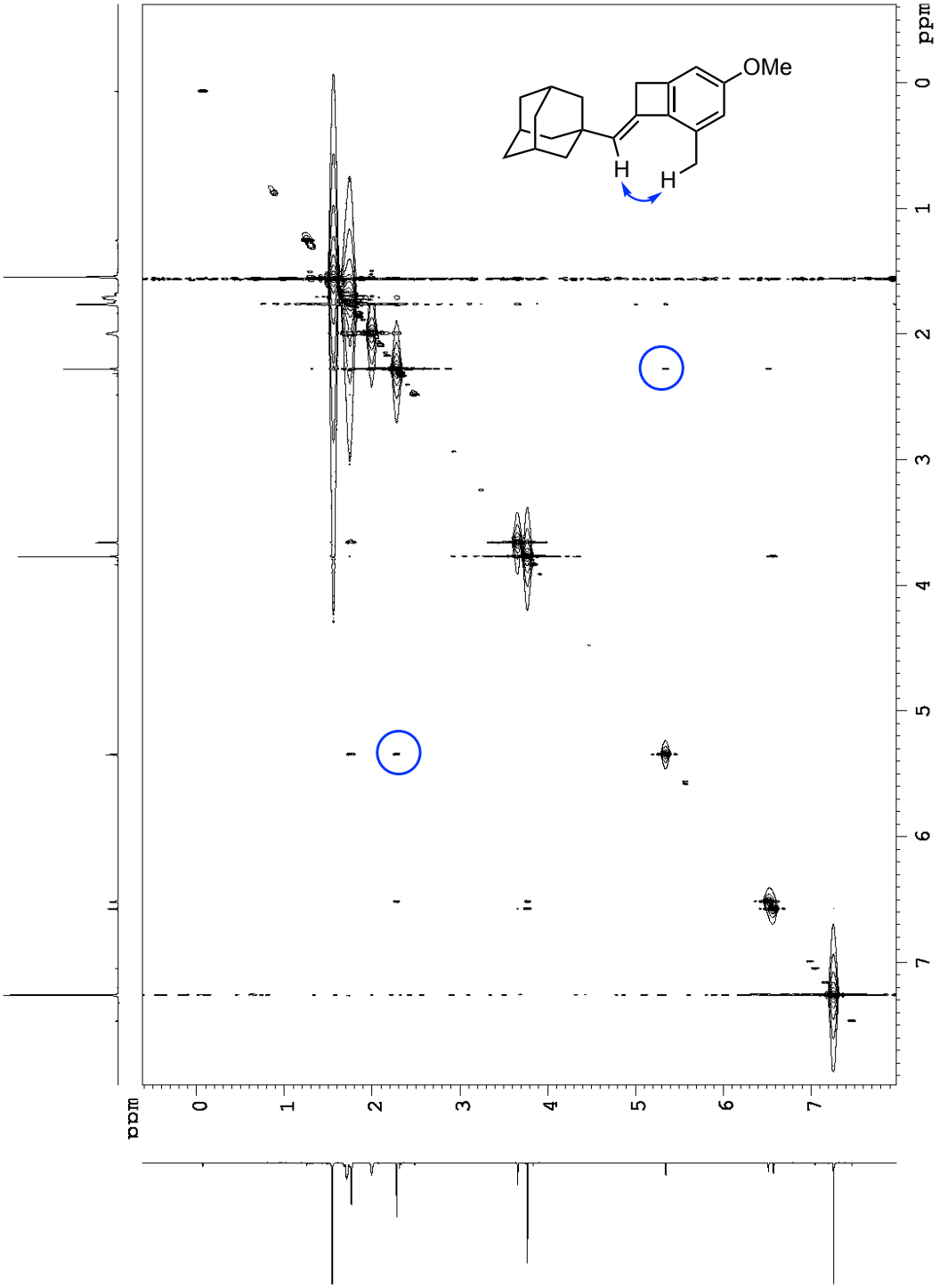

Figure S52. ^{1}H NMR (500 MHz, $CDCl_3$) of elimination product of ***trans*-ACB-4**.

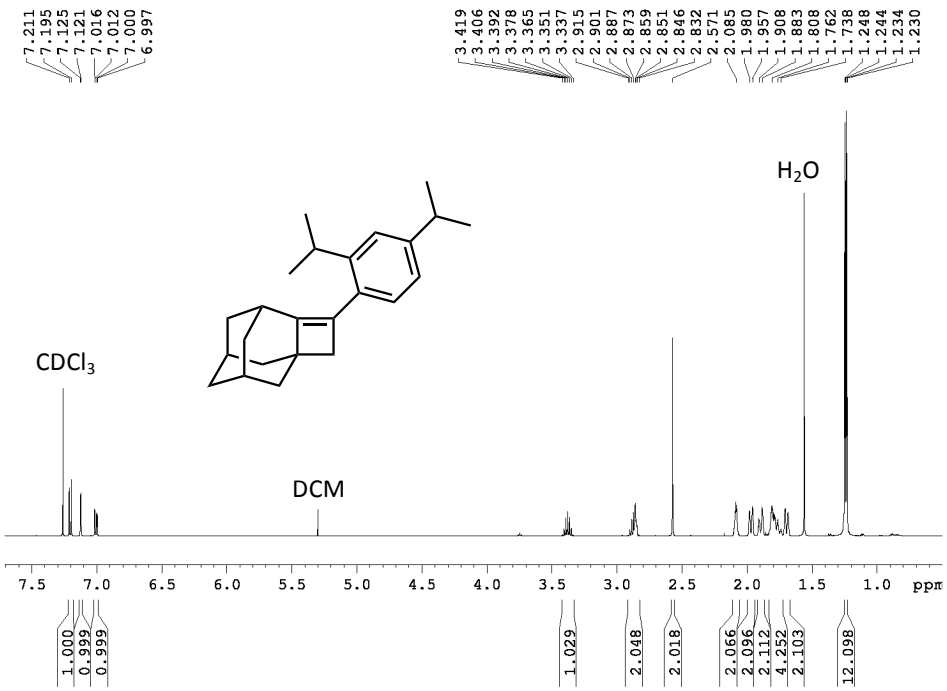

Figure S53. $^{13}C\{^{1}H\}$ NMR (126 MHz, $CDCl_3$) of elimination product of ***trans*-ACB-4**.

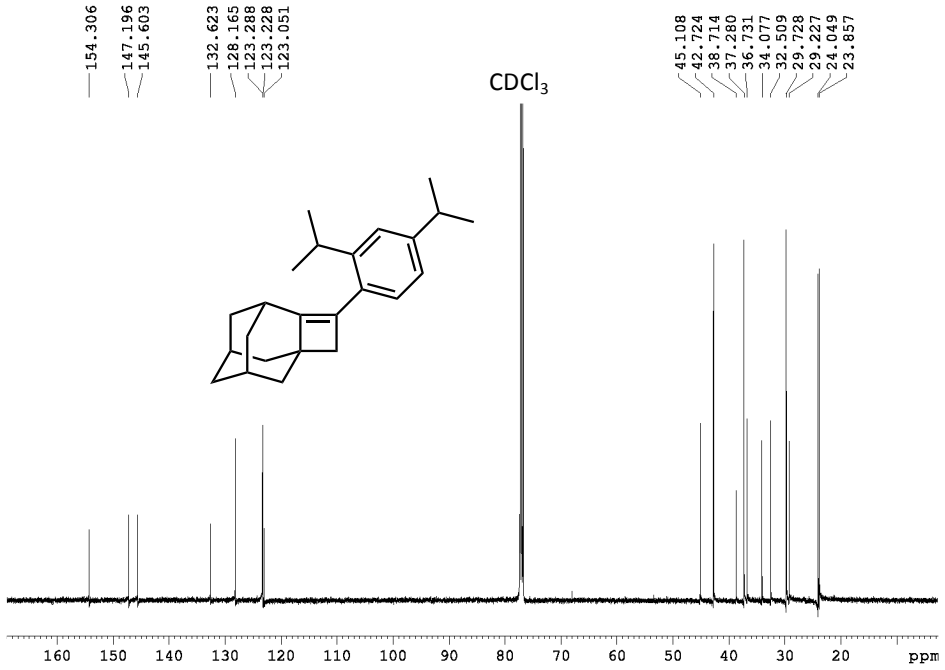

Figure S54. ^{1}H NMR (500 MHz, $CDCl_3$) of ***cis*-ACB-4**.

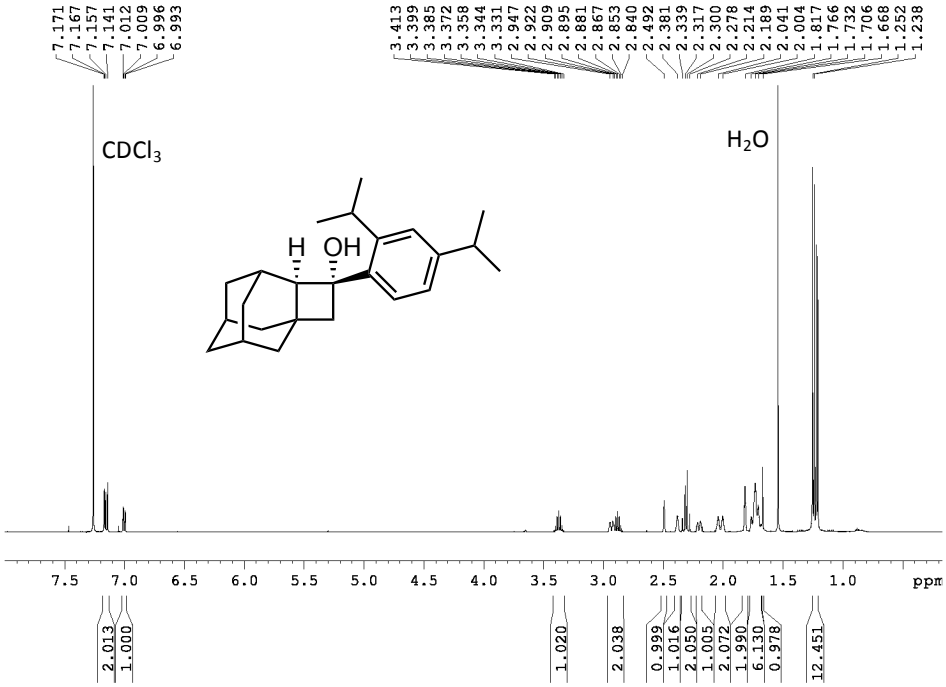

Figure S55. $^{13}C\{^{1}H\}$ NMR (126 MHz, $CDCl_3$) of ***cis*-ACB-4**.

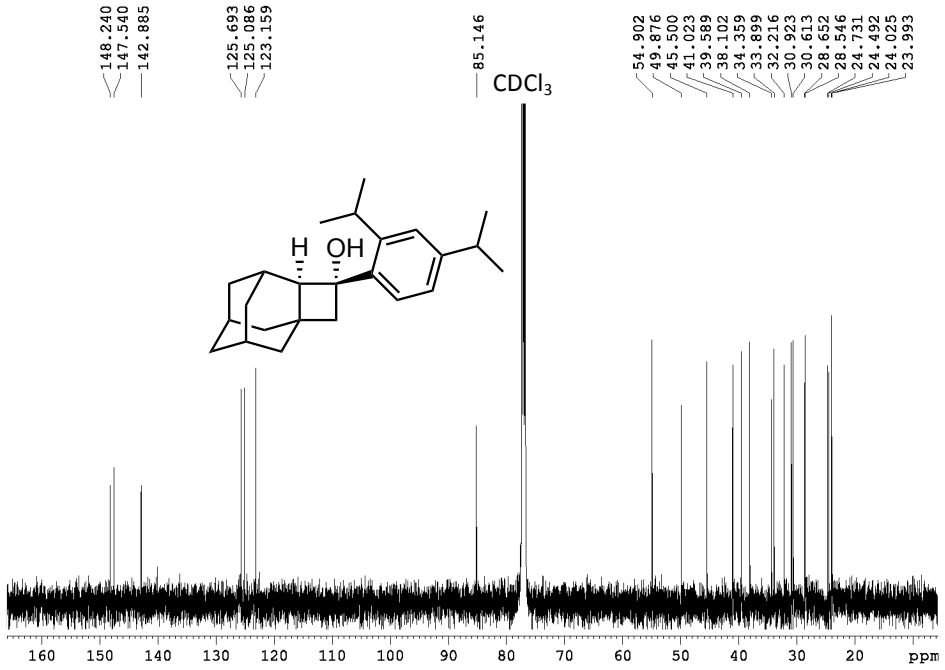

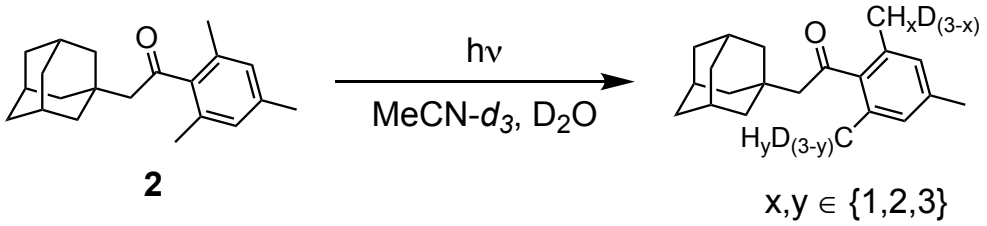

An oven-dried NMR tube was charged with **2** (5.2 mg) in MeCN-d_3 (0.9 mL) and D_2O (0.1 mL). The solution was sparged with argon and irradiated for 2 hrs. Partial deuteration of the indicated benzylic positions was confirmed by ^1H NMR spectroscopy (**Figure S56**), in which the integration of the peak corresponding to the methyl groups ortho to the ketone (δ 2.13) was reduced by a percentage as indicated in **Table S1**.

Figure S56. ^1H NMR (500 MHz, $CDCl_3$) of **2** (recovered starting material) after 2 hrs. irradiation in MeCN-d_3 : D_2O (9:1).

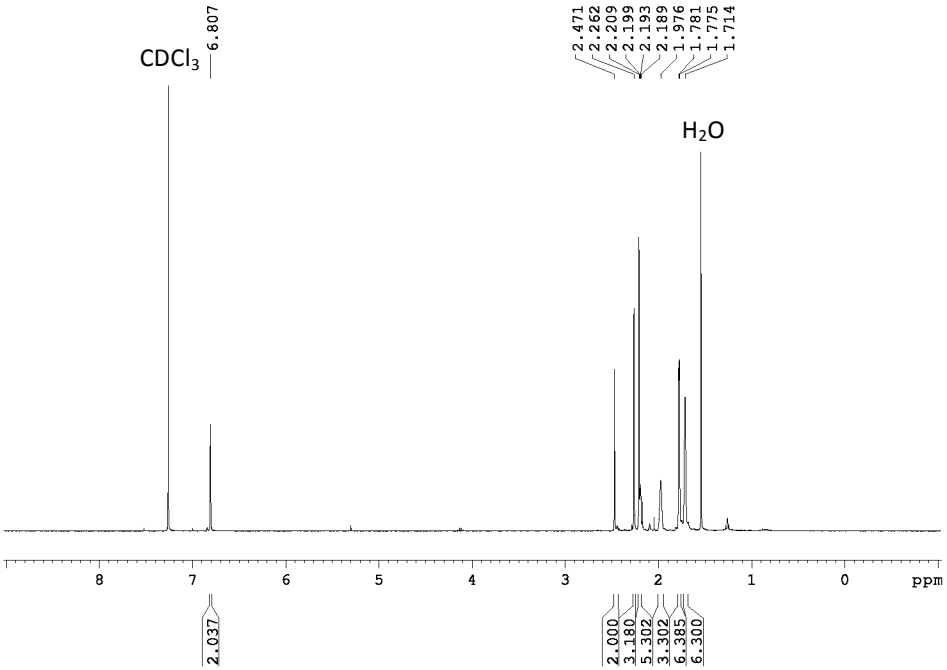

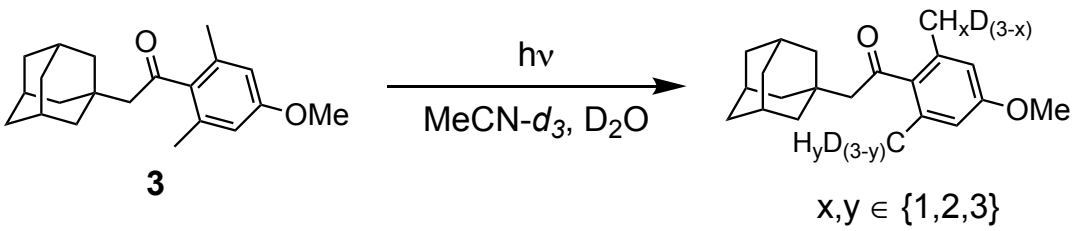

3

An oven-dried NMR tube was charged with **3** (5.5 mg) in MeCN-d_3 (0.9 mL) and D_2O (0.1 mL). The solution was sparged with argon and irradiated for 2 hrs. Partial deuteration of the indicated benzylic positions was confirmed by ^1H NMR spectroscopy (**Figure S58**).

Figure S57. ^1H NMR (500 MHz, $CDCl_3$) of **3** (recovered starting material) after 2 hrs. irradiation in MeCN-d_3 : D_2O (9:1).

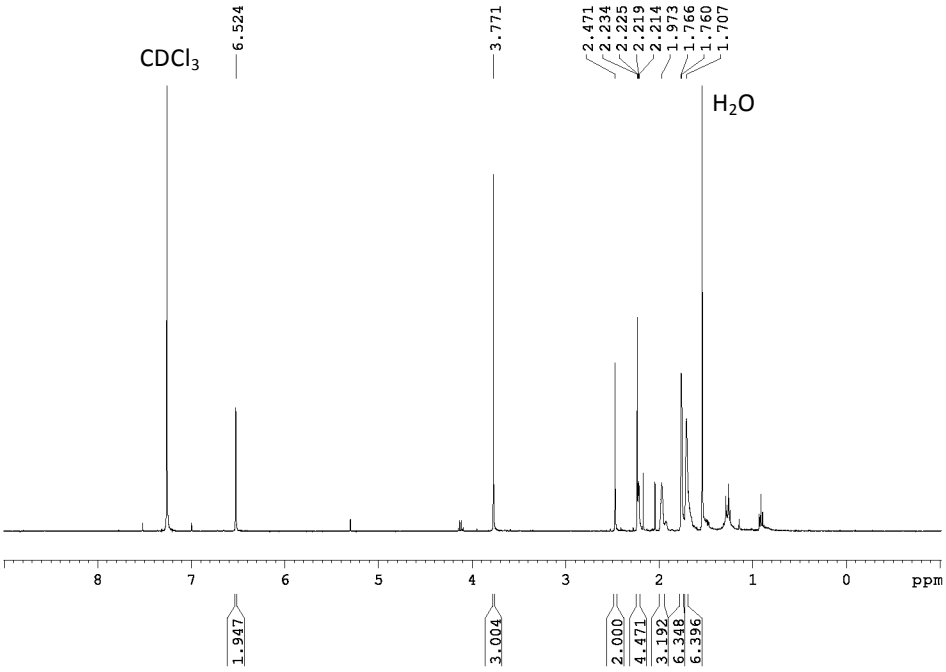

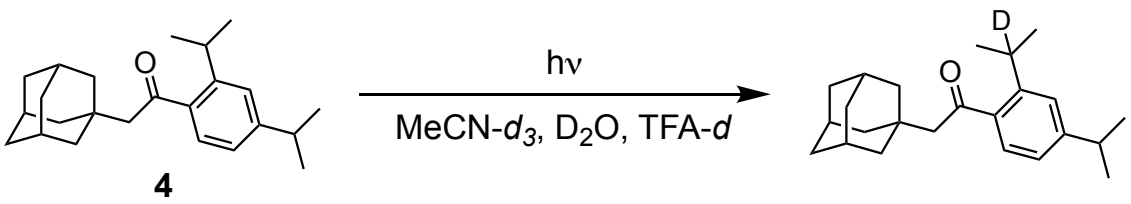

4

An oven-dried NMR tube was charged with **4** (5.9 mg) in MeCN-d_3 (0.8 mL), D_2O (0.1 mL), and TFA-*d* (0.1 mL). The solution was sparged with argon and irradiated for 2 hrs. Deuteration of the benzylic position is confirmed by ^{1}H NMR (**Figure S57**).

Figure S58. ^{1}H NMR (400 MHz, MeCN-d_3) of **4** after 2 hrs. irradiation in MeCN-d_3 : D_2O : TFA-*d* (8:1:1).

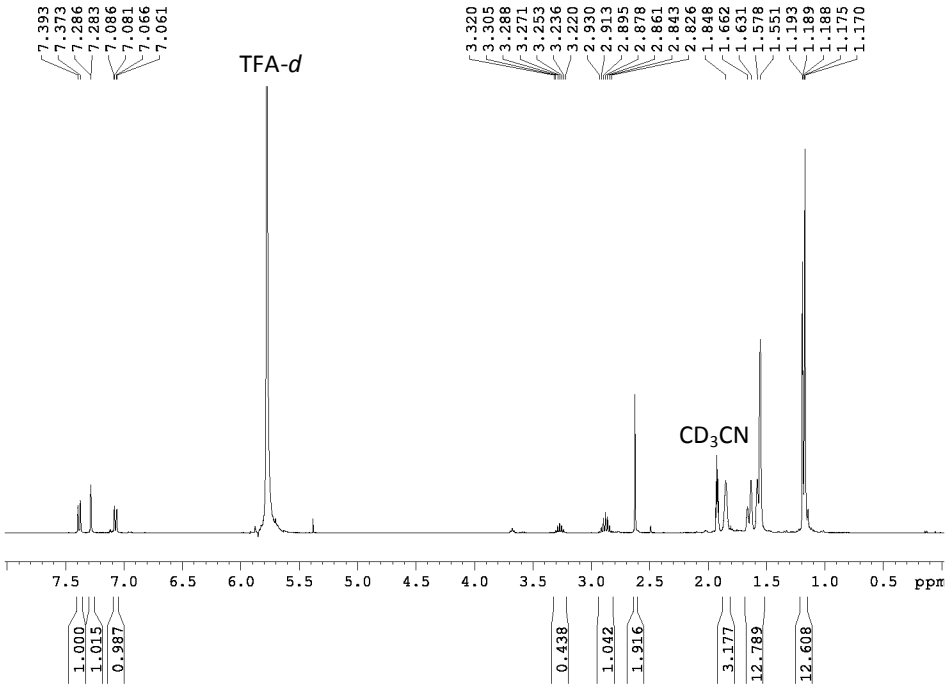

Figure S59. SEM micrographs and DLS unimodal size distribution analysis of nanocrystalline suspension of **1**.

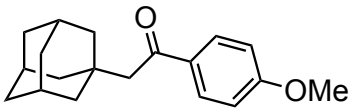

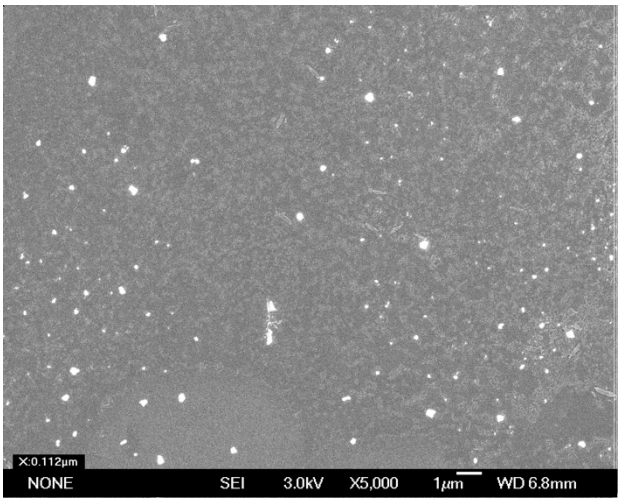

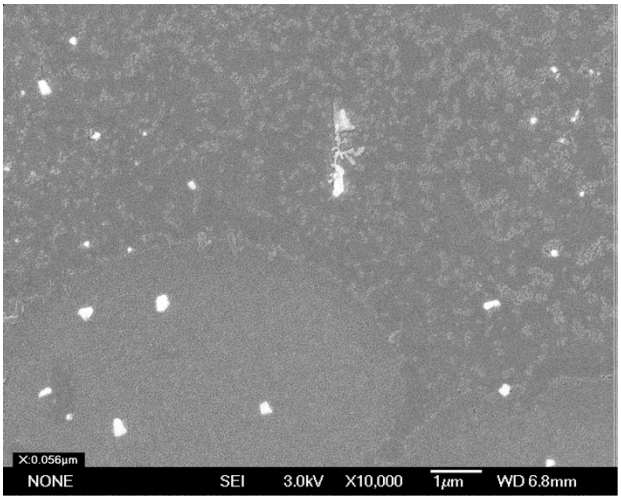

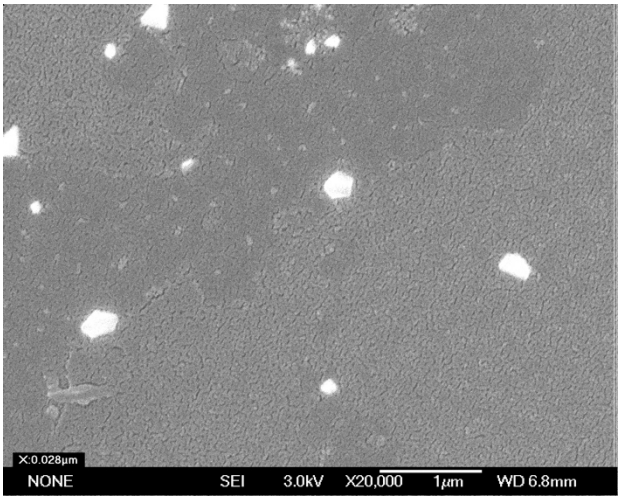

Unimodal Results Summary

Angle	Mean (nm)	Std.Dev (nm)	Baseline Error	P.I.	Counts/s	Diff.Coef (m²/s)	Overflow
90.0°	118.4	57.5	0.01%	2.114	3.03e+04	3.65e-12	0

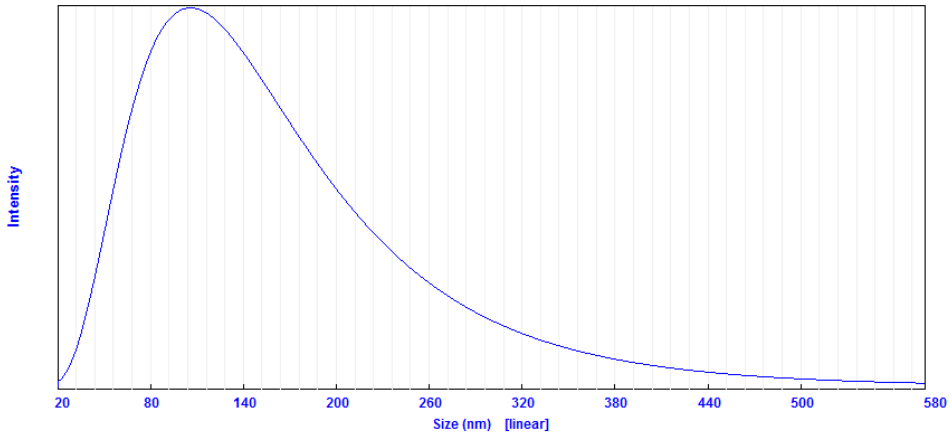

Figure S60. SEM micrographs and DLS unimodal size distribution analysis of nanocrystalline suspension of **2**.

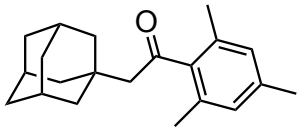

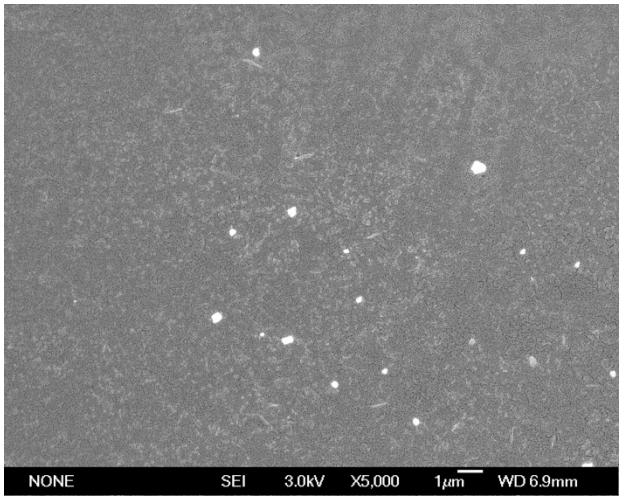

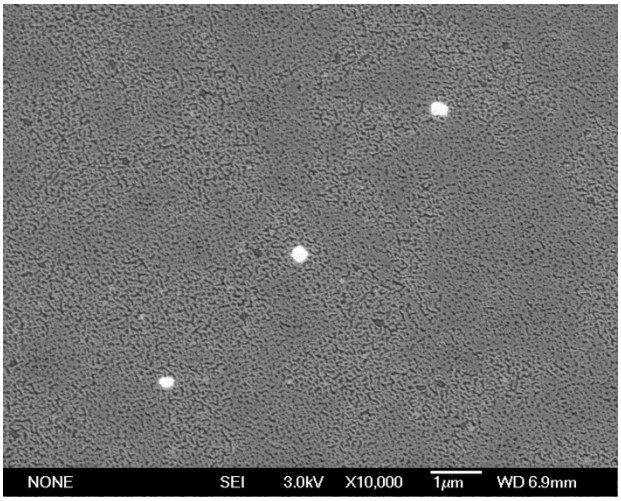

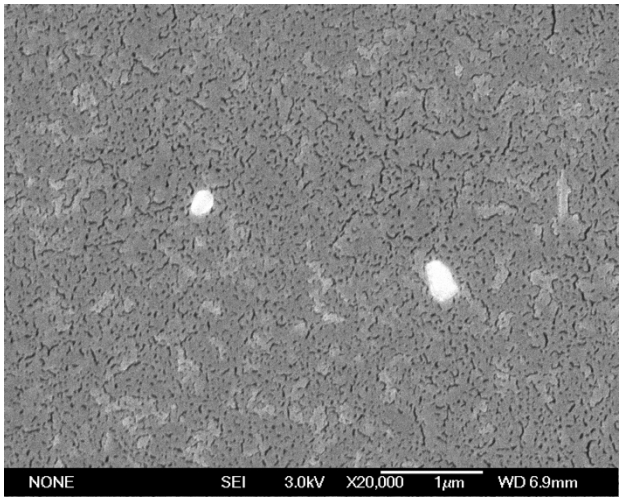

Unimodal Results Summary

Angle	Mean (nm)	Std.Dev (nm)	Baseline Error	P.I.	Counts/s	Diff.Coef (m²/s)	Overflow
90.0°	93.6	46.3	0.06%	6.307	7.35e+04	5.24e-12	0

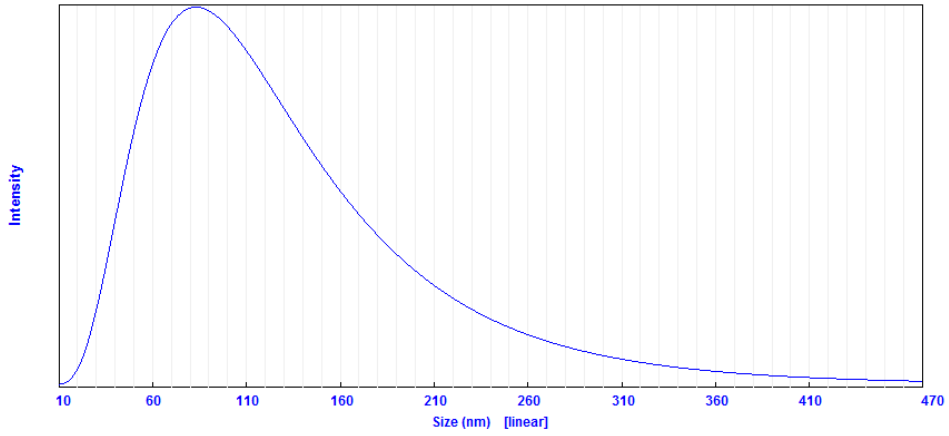

Figure S61. SEM micrographs and DLS unimodal size distribution analysis of nanocrystalline suspension of **3**.

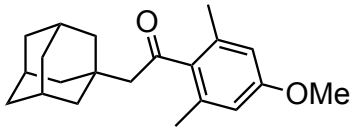

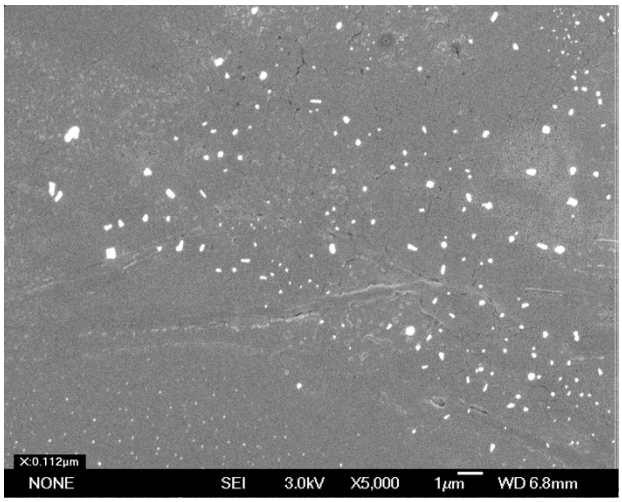

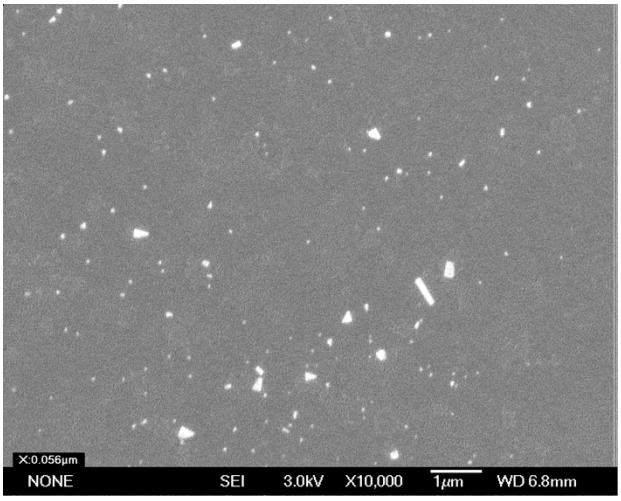

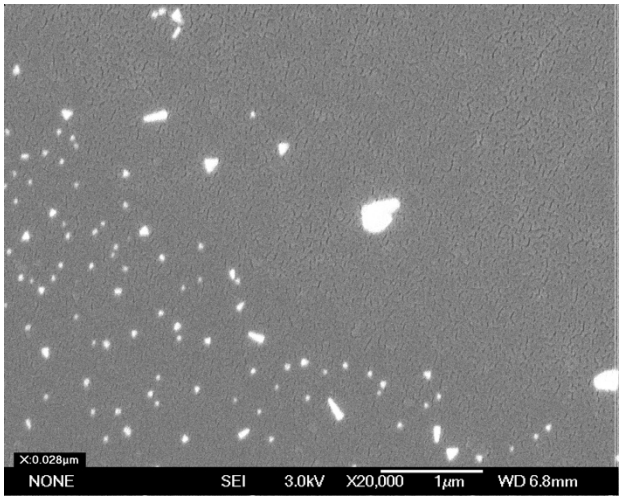

Unimodal Results Summary

Angle	Mean (nm)	Std.Dev (nm)	Baseline Error	P.I.	Counts/s	Diff.Coef (m^2/s)	Overflow
90.0°	201.9	98.7	0.04%	2.733	8.96e+03	2.43e-12	0

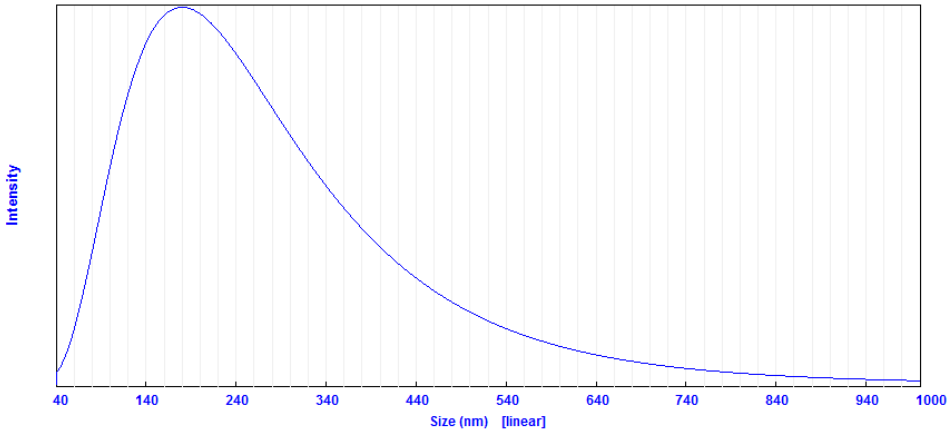

Figure S62. SEM micrographs and DLS unimodal size distribution analysis of nanocrystalline suspension of **4**.

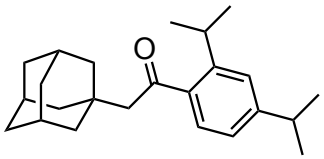

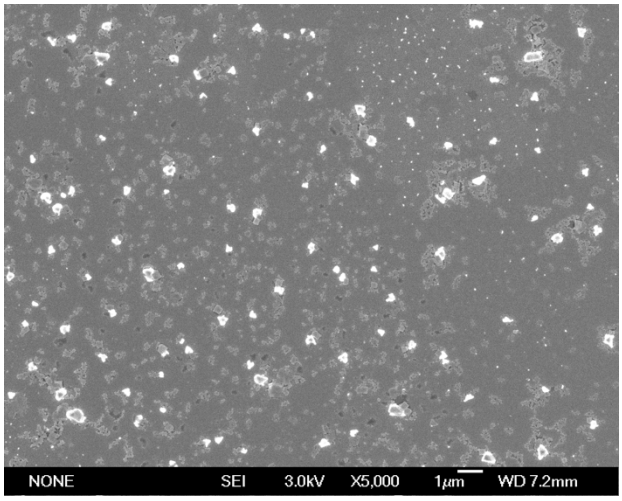

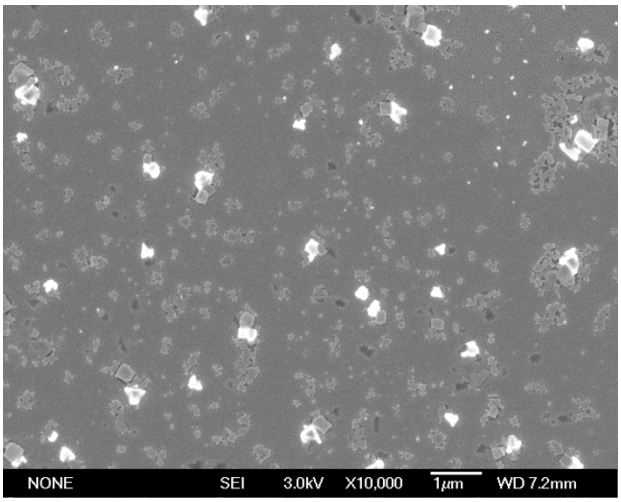

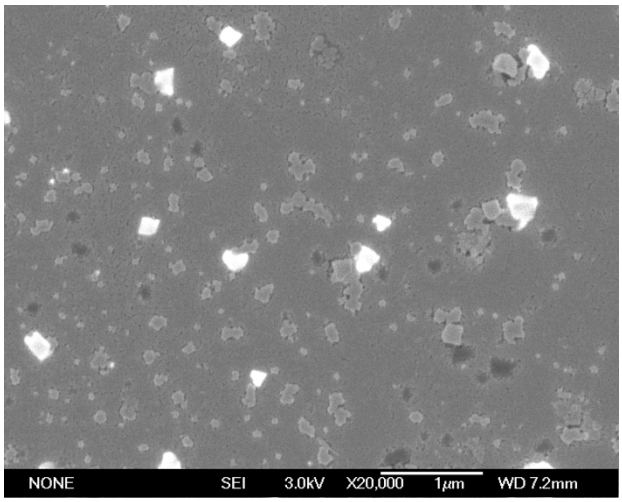

Unimodal Results Summary

Angle	Mean (nm)	Std.Dev (nm)	Baseline Error	P.I.	Counts/s	Diff.Coef (m^2/s)	Overflow
90.0°	255.6	121.6	0.07%	1.201	9.21e+03	1.92e-12	0

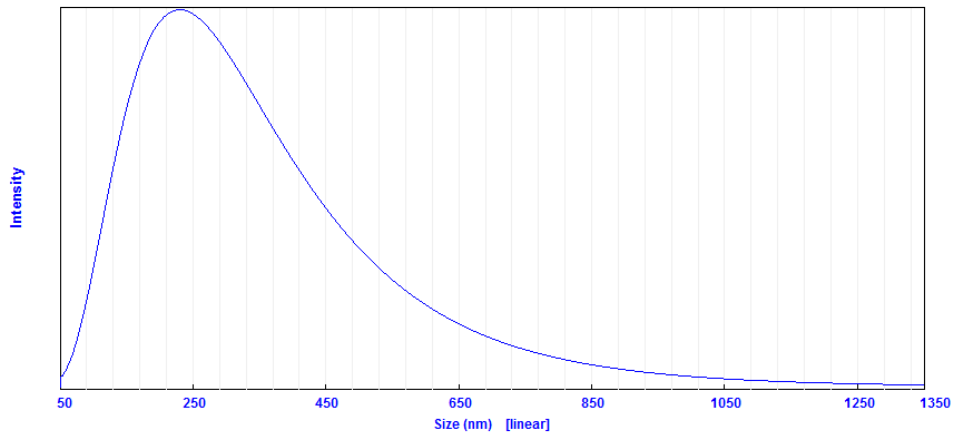

Figure S63. SEM micrographs and DLS unimodal size distribution analysis of nanocrystalline suspension of **5**.

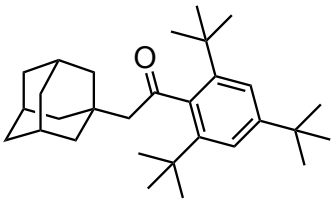

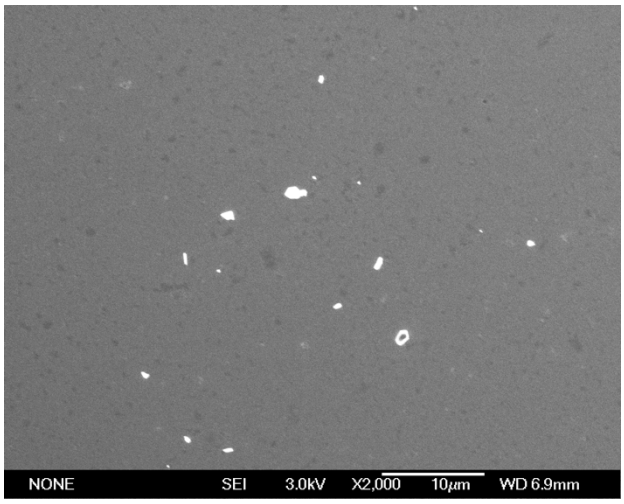

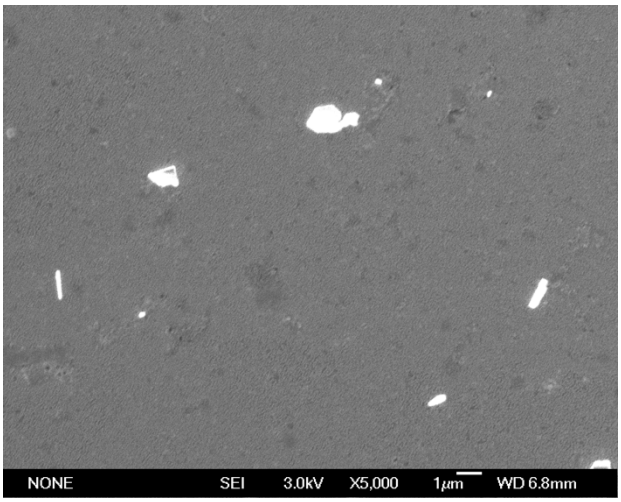

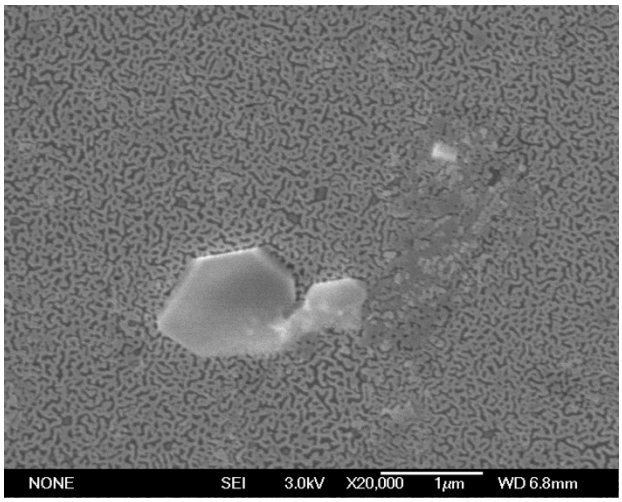

Unimodal Results Summary

Angle	Mean (nm)	Std.Dev (nm)	Baseline Error	P.I.	Counts/s	Diff.Coef (m^2/s)	Overflow
90.0°	487.9	239.0	0.00%	-2.962	6.76e+04	1.01e-12	2

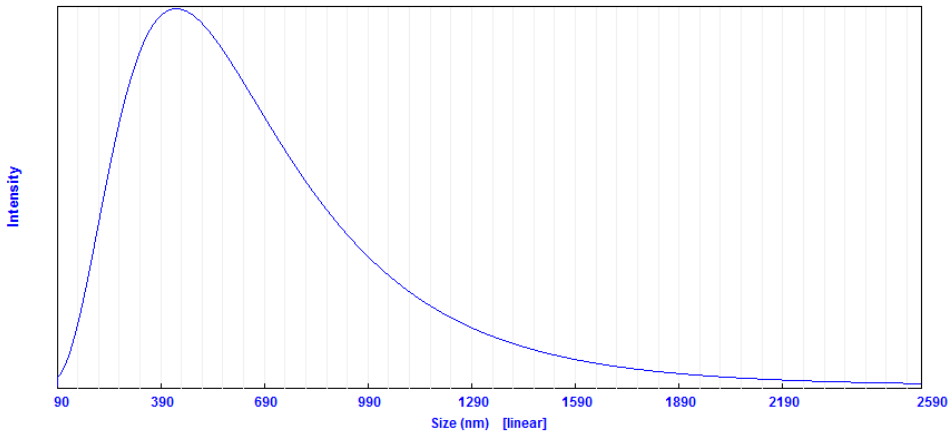

Figure S64. Simulated and experimental PXRD patterns of **1**.

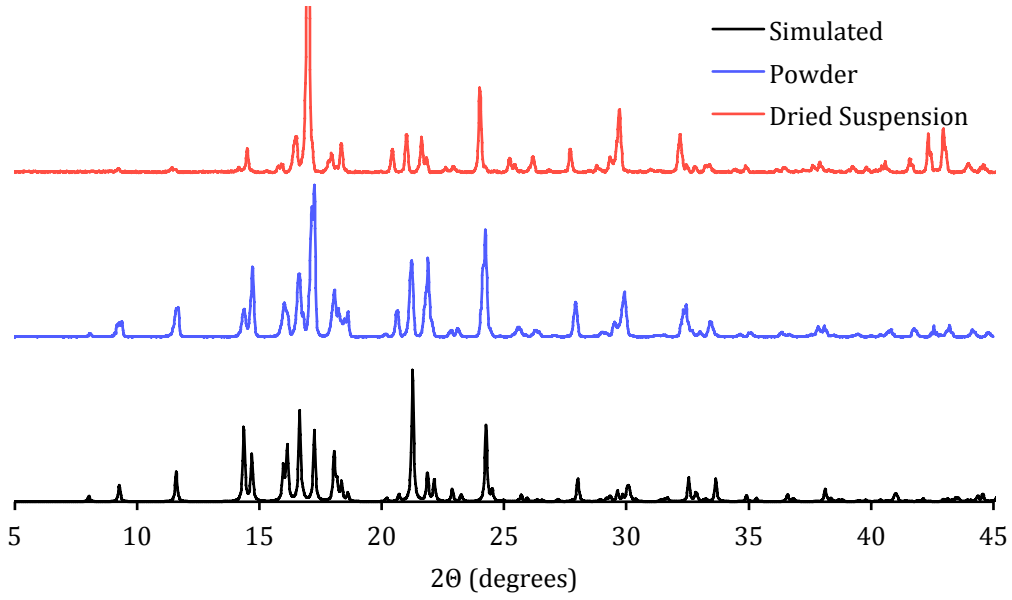

Figure S65. Simulated and experimental PXRD patterns of **2**.

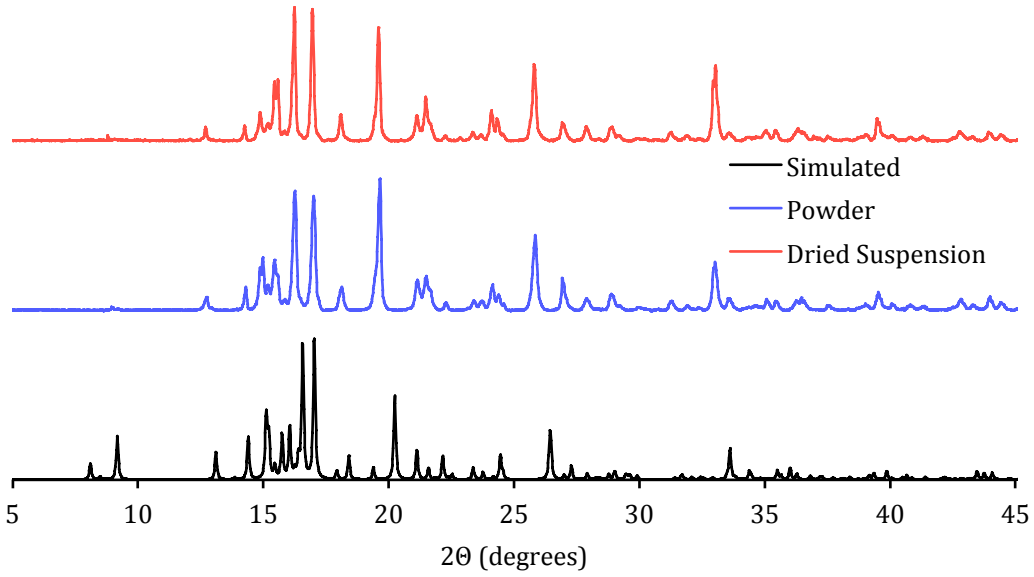

Figure S66. Simulated and experimental PXRD patterns of **3**.

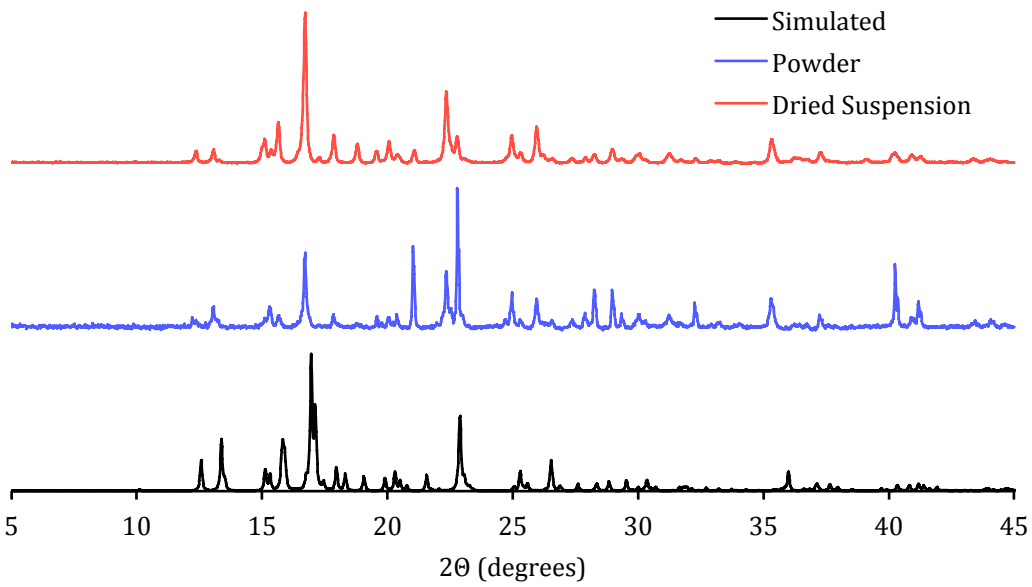

Figure S67. Simulated and experimental PXRD patterns of **4**.

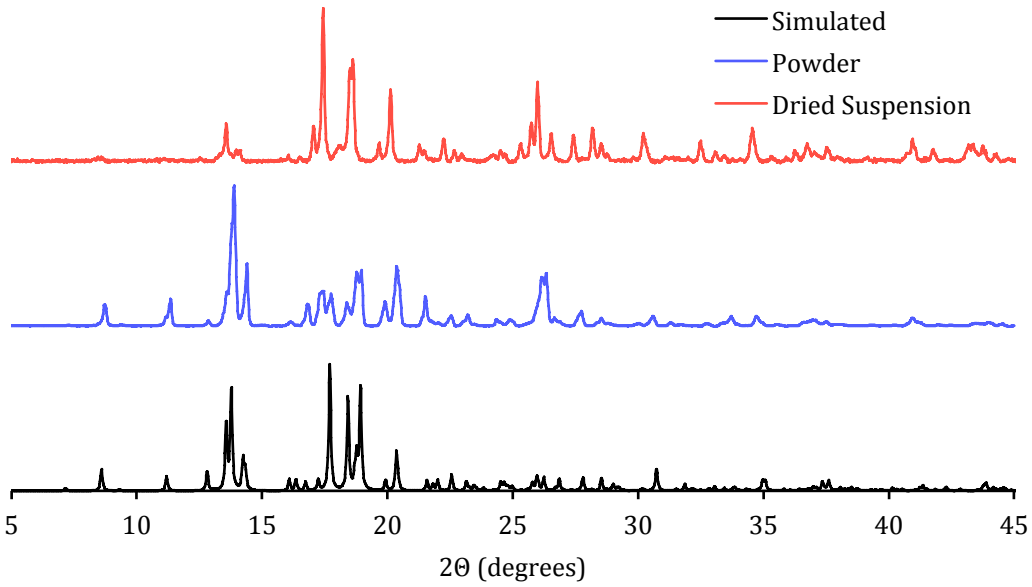

Figure S68. Simulated and experimental PXRD patterns of **5**.

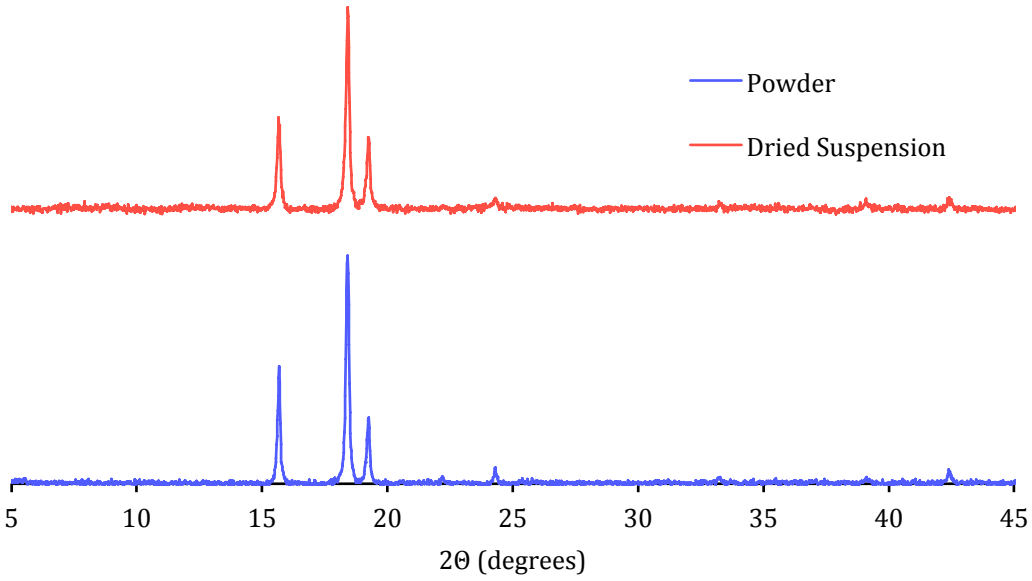

Figure S69. Transient absorption spectra of **1** : 0.01 mg/mL MeCN solution.

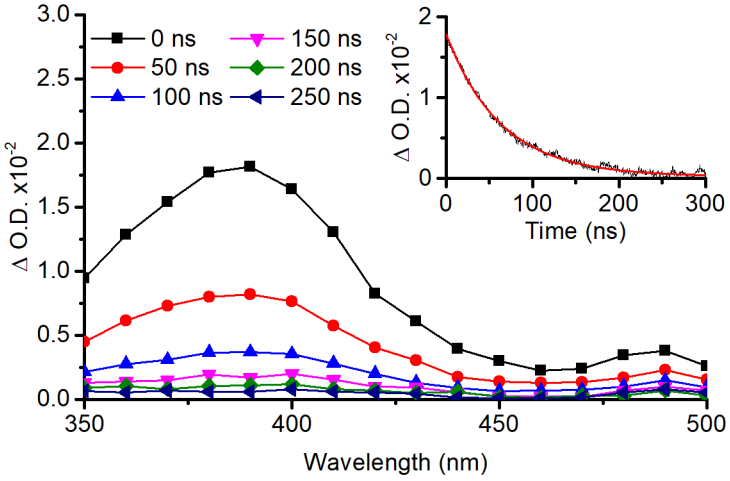

Figure S70. Transient absorption spectra of **1** : 0.01 mg/mL nanocrystalline suspension.

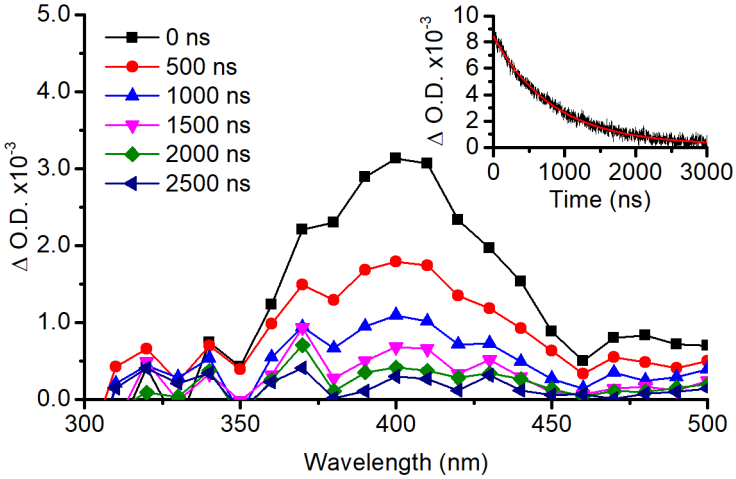

Figure S71. Transient absorption spectra of **3** : 0.02 mg/mL MeCN solution.

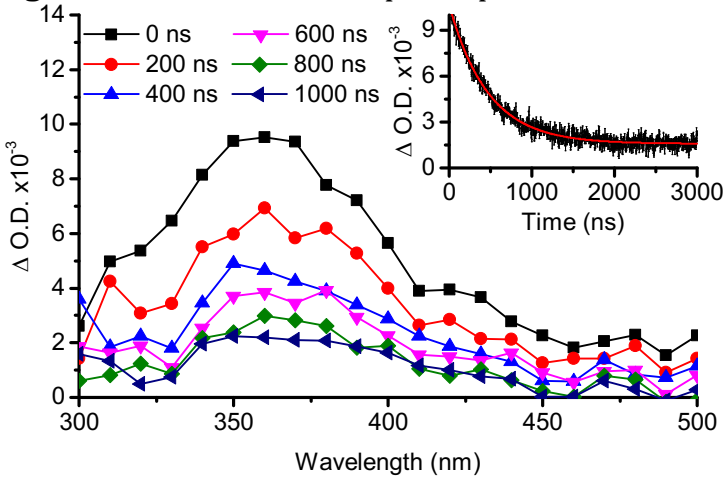

Figure S72. Transient absorption spectra of **4** : 0.025 mg/mL nanocrystalline suspension.

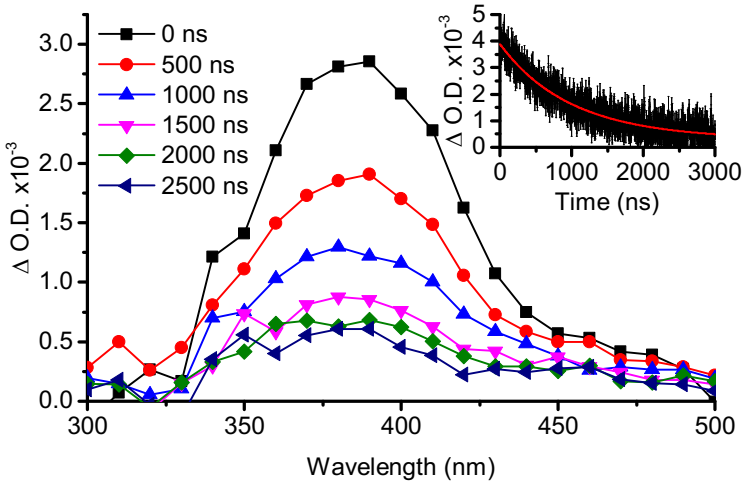

Figure S73. Transient absorption spectra of **5** : 0.05 mg/mL MeCN solution.

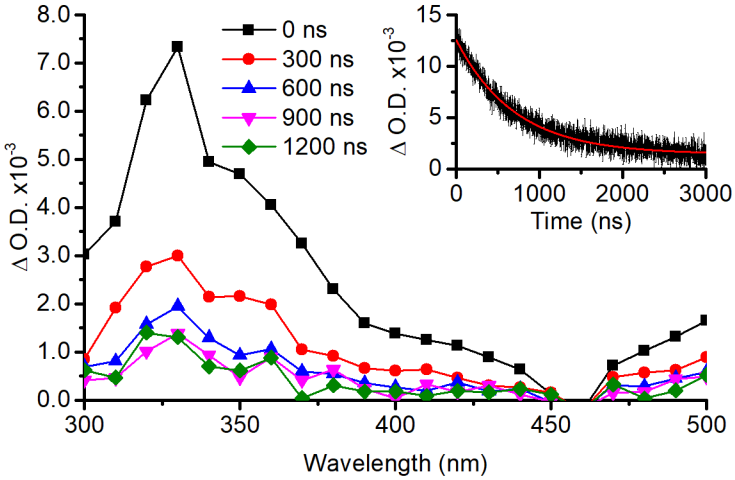

Table S2. Selected crystal structure data for ketones 1-4.[a]

Ketone	1[b]	2	3	4
Space Group	$P2_1/m$	$P\bar{1}$	$P\bar{1}$	Pbca
a (Å)	6.417	6.819	6.873	7.678
b (Å)	21.991	11.296	10.713	20.557
c (Å)	10.566	11.941	12.302	24.693
α (°)	90.00	112.70	77.26	90
β(°)	90.02	97.57	74.20	90
γ(°)	90.00	90.14	87.04	90
Z	4	2	2	8
Volume ($Å^3$)	1491.0(3)	839.74	849.9(6)	3897.7(9)
GoF	1.039	1.132	1.011	1.035
R (%)	4.17	4.73	4.58	7.39
Rw (%)	10.60	11.75	12.21	14.48

[a]Crystals of **2**, **3**, and **4** were obtained by slow evaporation of ethanol solutions. X-ray diffraction data was acquired on a Bruker Smart ApexII CCD-single crystal X-ray Diffractometer.
[b]Data obtained from reference 7.

Figure S74. Crystal structure of **2** with thermal ellipsoids drawn at the 50% probability level.

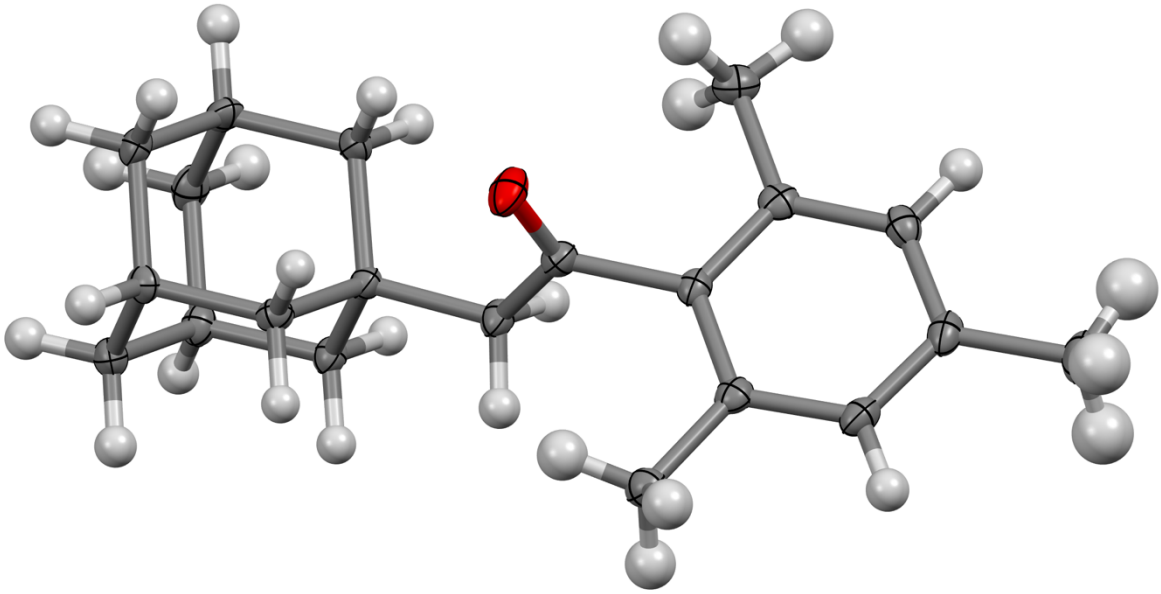

Figure S75. Crystal structure of **3** with thermal ellipsoids drawn at the 50% probability level.

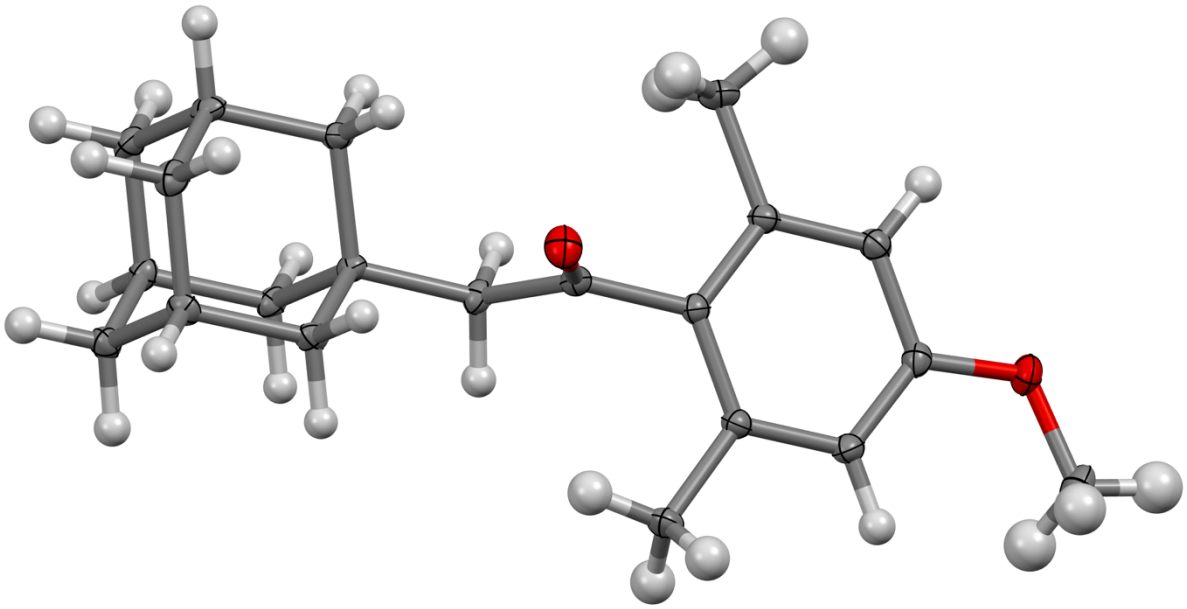

Figure S76. Crystal structure of **4** with thermal ellipsoids drawn at the 50% probability level.

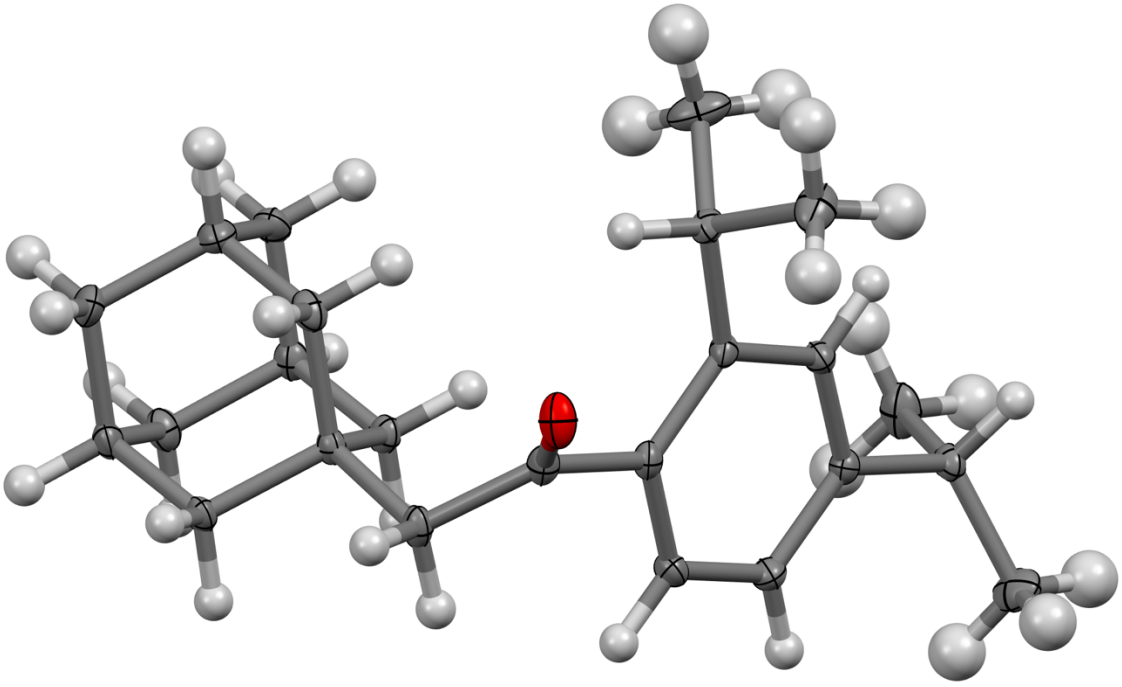

Computational Details: The calculated structure of **5** was produced using the Spartan '16 program. A conformational search using the force-field method MMFF resulted in 6 conformers with energies within 2 kcal/mol. These conformers were nearly identical, differing only by rotation of the t-butyl groups. Conformers in which the adamantane group was placed closer to the aromatic ring displayed much higher energies (>30 kcal/mol increase). The lowest energy conformer was submitted to the DFT method B3LYP/6-31G* for equilibrium geometry calculation. The structure obtained from this calculation is shown in Figure S77 and the corresponding atomic positions are listed in Table S3.

Figure S77. Calculated Structure of **5**.

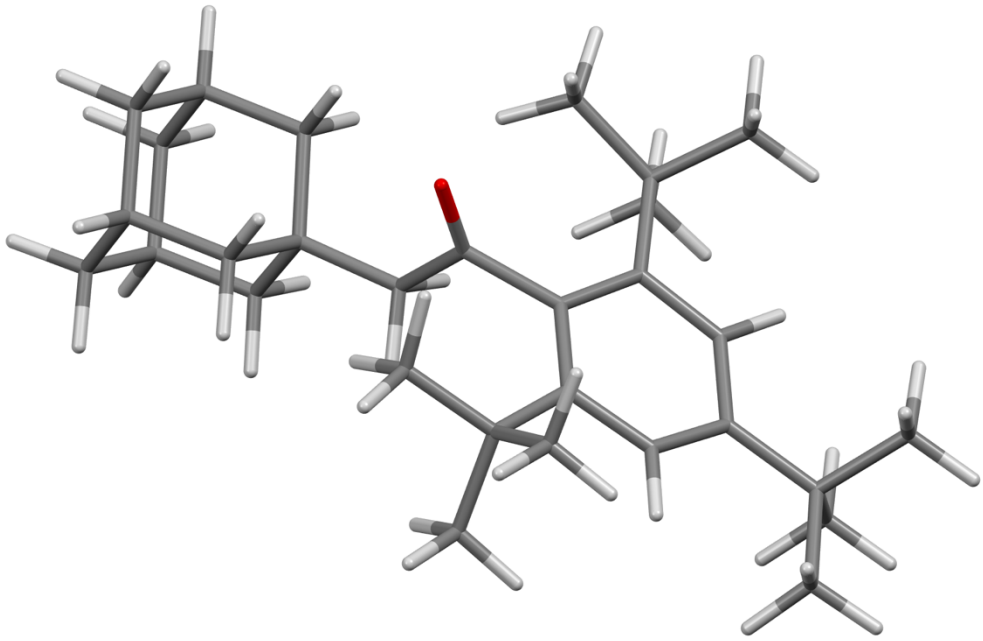

Table S3. Cartesian Coordinates for Calculated Structure of 5.

C	1.3027	0.8005	1.4405
C	0.9097	-1.7296	2.561
C	2.284	0.1651	2.2103
C	0.0979	0.0833	1.1698
C	-0.1274	-1.1772	1.7892
C	2.1347	-1.1059	2.764
C	3.2809	-1.7399	3.5732
C	4.5371	-1.8598	2.6783
C	3.6098	-0.8472	4.7936
C	2.9259	-3.1466	4.0915

C	1.6841	2.2477	0.9848
C	2.1594	3.0563	2.2243
C	0.5591	3.0974	0.3632
C	2.8423	2.1677	-0.0398
C	-1.4154	-2.064	1.7467
C	-1.0794	-3.4168	1.0673
C	-1.8762	-2.3245	3.2068
C	-2.6484	-1.4909	1.0244
C	-0.872	0.6011	0.1054
O	-1.8366	1.2965	0.3634
H	-3.4717	-2.2058	1.1379
H	-2.9707	-0.535	1.4413
H	-2.4943	-1.3626	-0.0483
H	-2.1226	-1.3811	3.7065
H	-2.7761	-2.951	3.2027
H	-1.9579	-4.0735	1.0801
H	-0.788	-3.268	0.0205
H	0.7436	-2.6988	3.0112
H	3.2165	0.6883	2.3854
H	2.06	-3.1284	4.7629
H	3.7714	-3.5559	4.6559
H	2.7077	-3.841	3.2718
H	2.7409	-0.7478	5.4544
H	4.4311	-1.2858	5.3733
H	3.9154	0.1601	4.4914
H	5.3685	-2.2958	3.2457
H	4.8653	-0.8845	2.3041
H	1.3703	3.103	2.9834
H	-0.3101	3.1747	1.0206
H	0.2222	2.7257	-0.6041
H	0.9456	4.1087	0.1904
H	2.3968	4.083	1.9219
H	3.1639	3.1758	-0.3289
H	2.5295	1.643	-0.9504
H	4.3435	-2.5019	1.8113
H	3.0549	2.6458	2.6983
H	3.7124	1.6392	0.3632
H	-0.2608	-3.9457	1.5653
H	-1.1232	-2.8368	3.8114
C	-0.4975	0.1532	-1.3123

C	-1.3543	0.5701	-2.5287
H	0.5417	0.4797	-1.4714
H	-0.4222	-0.9449	-1.2774
C	-0.6766	-0.0265	-3.7922
C	-1.43	2.1077	-2.7099
C	-2.7984	0.014	-2.4523
C	-3.5905	0.3735	-3.7265
C	-2.2218	2.4688	-3.9844
C	-1.4629	0.3299	-5.0678
H	0.353	0.353	-3.8712
H	-0.6033	-1.1192	-3.6897
H	-2.7686	-1.0796	-2.3358
H	-3.3013	0.4218	-1.5688
H	-0.9572	-0.1082	-5.939
H	-0.4128	2.5191	-2.7843
H	-1.9038	2.5618	-1.8337
C	-3.6536	1.9064	-3.8749
C	-1.5247	1.8627	-5.2179
C	-2.8939	-0.2343	-4.9601
H	-0.5102	2.2739	-5.3203
H	-2.0699	2.1315	-6.1335
H	-2.2613	3.5619	-4.083
H	-4.2363	2.1765	-4.7667
H	-4.1665	2.3481	-3.0097
H	-3.4635	-0.0022	-5.8709
H	-2.8621	-1.3297	-4.8745
H	-4.6082	-0.0303	-3.6403